Chiral Rhodium(I) and Iridium(I) Amino−Olefin Complexes: pK_a, N−H Bond Dissociation Energy, and Catalytic Transfer Hydrogenation

Pascal Maire, Frank Breher, Hartmut Schönberg, and Hansjörg Grützmacher*

Department of Chemistry and Applied Biosciences, ETH-Hönggerberg, HCI H131, CH-8093 Zürich, Switzerland

Received February 10, 2005

The chiral tetrachelating amino−olefins (*R*,*R*)-*N*,*N*′-bis(5*H*-dibenzo[*a*,*d*]cyclohepten-5-yl)-1,2-diaminocyclohexane ((*R*,*R*)-trop$_2$dach) and (*S*,*S*)-*N*,*N*′-bis(5*H*-dibenzo[*a*,*d*]cyclohepten-5-yl)-1,2-diphenyl-1,2-ethylenediamine ((*S*,*S*)-trop$_2$dpen) were prepared and used as ligands in the complexes (*R*,*R*)-[Rh(trop$_2$dach)]OTf and (*S*,*S*)-[Rh(trop$_2$dpen)]OTf (OTf$^-$ = $CF_3SO_3^-$). Quasi-reversible reductions, d^8-[Rh^I(trop$_2$diamine)]$^+$ + e$^-$ → d^9-[Rh^0(trop$_2$diamine)] and d^9-[Rh^0(trop$_2$diamine)] + e$^-$ → d^{10}-[Rh^{-I}(trop$_2$diamine)]$^-$, at rather negative potentials (trop$_2$diamine = trop$_2$dach, $E_{1/2}^1$ = −1.83 V, $E_{1/2}^2$ = −2.27 V; trop$_2$diamine = trop$_2$dpen, $E_{1/2}^1$ = −1.78 V, $E_{1/2}^2$ = −2.24 V; vs Fc$^+$/Fc) indicate the donor capacity of the amine functions. One NH group in (*R*,*R*)-[Rh(trop$_2$dach)]OTf (pK_a = 15.7(2), NH bond dissociation energy (BDE) 317(2) kJ mol^{-1}) is easily deprotonated to give the neutral amide (*R*,*R*)-[Rh(trop$_2$dach-H)], which is quasi-reversibly oxidized at $E°$ = −0.34 V (vs Fc/Fc$^+$) to the radical cation (*R*,*R*)-[Rh(trop$_2$dach-H)]$^{\bullet+}$. The pK_a and BDE values of the NH group in these 16-electron complexes are lower than in related pentacoordinated 18-electron complexes. X-ray diffraction analyses show that the rhodium complexes have distorted-square-planar structures. The Rh−N bond shortens by about 7% upon deprotonation. The rhodium complexes are inactive as catalysts for transfer and direct hydrogenation of ketones. However, the distorted-trigonal-bipyramidal iridium complex (*S*,*S*)-[IrCl(CO)(trop$_2$dpen)], where the amino−olefin ligand serves as a tridentate ligand, serves as a chiral precursor to an active phosphane-free catalyst in the transfer hydrogenation of acetophenone with 2-propanol, and the *R* isomer of 1-phenylethanol was obtained in 82% ee (>98% conversion when acetophenone:KO*t*Bu:cat = 1:0.1:0.01, T = 80 °C, reaction time 1 h).

Introduction

Nitrogen compounds are highly attractive as ligands for transition-metal complexes, and their application in catalysis has become a major research topic.[1−3] Amines do not suffer from the intrinsic drawbacks of phosphanes, especially their oxygen sensitivity.[4] Moreover, biological systems are an (almost) inexhaustible source of chiral nitrogen compounds. However, late-transition-metal amine complexes are often not very stable and the amine is rather easily displaced by stronger σ-donors (phosphanes, arsanes, etc.).[5] Complexes with sp^2 valence electron configured nitrogen donors seem to have a higher stability.[5a] A number of rhodium and iridium complexes [M(cod)(N)$_2$]$^+$ and [M(cod)(NN)]$^+$ with various N = monodentate and NN = bidentate N-bonded ligands could be prepared, structurally characterized,[6] or thoroughly characterized by NMR spectroscopy.[7]

A major reference covering the literature up to 1978 does not cite any example of a stable rhodium or iridium amide, [M(NR$_2$)L$_n$] (M = Rh, Ir; L = coligand).[8] Meanwhile, there has been considerable progress in the isolation and understanding of these compounds.[9] Apart from binuclear compounds with bridging amides,[10] a variety of mononuclear compounds[4a,6f,g,11,12a,16e,f] were isolated. Often they contain a reactive M−N bond susceptible to insertion reactions.[9,11a,i,12] The M−N bond is covalent but highly polar,[13] and depending on the structure and electronic configuration, the interaction of metal-localized π orbitals with the lone pair at the

* To whom correspondence should be addressed. E-mail: gruetzmacher@inorg.chem.ethz.ch.

(1) For recent work using chiral Rh(I) diamine complexes in asymmetric hydrogenations, see: (a) Jones, M. D.; Raja, R.; Thomas, J. M.; Johnson, B. F. G.; Lewis, D. W.; Rouzaud, J.; Harris, K. D. M. *Angew. Chem., Int. Ed.* **2003**, *42*, 4326, and literature cited therein. (b) Raja, R.; Thomas, J. M.; Jones, M. D.; Johnson, B. F. G.; Vaughan, D. E. W. *J. Am. Chem. Soc.* **2003**, *125*, 14983, and literature cited therein.

(2) Review: Fache, F.; Schulz, E.; Tommasino, M. L. Lemaire, M. *Chem. Rev.* **2000**, *100*, 2159.

(3) Review: Togni, A.; Venanzi, L. M. *Angew. Chem., Int. Ed. Engl.* **1994**, *33*, 497.

(4) In contrast, amine rhodium complexes can be used in oxygenation chemistry; for recent examples see: (a) de Bruin, B.; Kicken, R. J. N. A. M.; Suos, N. F. A.; Donners, M. P. J.; den Reijer, C. J.; Sandee, A. J.; de Gelder, R. Smits, J. M. M.; Gal, A. W.; Spek, A. L. *Eur. J. Inorg. Chem.* **1999**, 1581 and literature cited therein. (b) de Bruin, B.; Brands, J. A.; Suos, N. F. A.; Donners, J. J. J. M.; Donners, M. P. J.; de Gelder, R.; Smits, J. M. M.; Gal, A. W.; Spek, A. L. *Chem. Eur. J.* **1999**, *5*, 2921 and literature cited therein.

(5) There are too many references to cite here. For a recent paper discussing the displacement of an amine by an imine in an iridium cod complex as a key step in the catalytic cycle for imine hydrogenations see: (a) Dorta, R.; Broggini, D.; Kissner, R. Togni, A. *Chem. Eur. J.* **2004**, *10*, 4546 and literature cited therein. For early investigations relevant to our work see: (b) Uson, R., Oro, L. A.; Claver, C., Garralda, M. A. *J. Organomet. Chem.* **1976**, *105*, 365. (c) Cocevar, C.; Mestroni, G.; Camus, A. *J. Organomet. Chem.* **1972**, *35*, 389.

10.1021/om0500927 CCC: $30.25
Publication on Web 05/24/2005

nitrogen center may be stabilizing or destabilizing.[14] Rhodium and iridium amides play a crucial role in catalyzed hydroaminations,[15] imine hydrogenations,[5a] and (transfer) hydrogenations.[16] In the last type of reaction, the M−N bond may serve as a "metal−ligand-bifunctional" entity (*ML-bi* mechanism).[17]

Chart 1. Examples of Isolated Rhodium(I) and Iridium(I) Complexes with Amino−Olefin Ligands (A, B)[a]

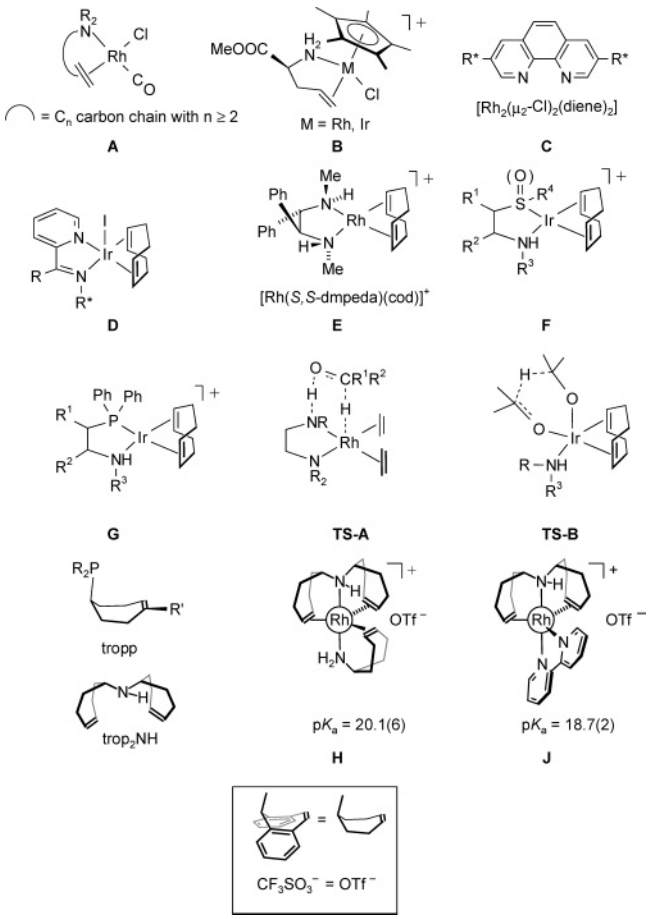

A B C D E F G TS-A TS-B H J

[a] Complexes **C**−**G** are examples of catalyst precursors used in catalytic transfer hydrogenations proceeding via the transition states **TS-A** and **TS-B**. Complexes **H** and **J** contain the new rigid amino−olefin ligand trop$_2$NH.

Many of the complexes cited above contain olefins as additional ligands (mostly cod = η^4-1,5-cyclooctadiene). Like amines, olefins are generally considered to be rather weakly binding ligands. Isolated complexes containing a chelating amino−olefin ligand, as in compounds **A** and **B** in Chart 1, are rare,[18] and some of these were indeed found to be labile. On the other hand, rhodium and iridium complexes with nitrogen donor molecules and olefins as ligands were discovered for homogeneously catalyzed transfer hydrogenation about 10 years ago. Gladiali et al. reported the use of mixtures of chiral phenanthrolines with rhodium(I) diene complexes **C** in enantioselective transfer hydrogenations.[19] Chiral Schiff-base iridium complexes such as **D** were employed successfully by Zassinovich for the same purpose.[20] At first, solvate complexes of the type [M(NN)(solv)]$^+$ (M = Rh, Ir) were assumed to be the catalytically active species (NN = chelating nitrogen ligand,

(6) For some selected examples of structurally characterized complexes relevant to this work, see: (a) [Rh(cod)(1,1′-binap-2,2′-$(NH_2)_2$]$^+$: Jones, M. D.; Almeida Paz, F. A.; Davies, J. E.; Johnson, B. F. G. *Acta Crystallogr.* **2003**, *E59*, m6. (b) [Rh(cod)(pyrazolylamine)] complexes: Esquius, G.; Pons, J.; Yáñez, R.; Ros, J.; Mathieu, R.; Donnadieu, B.; Lugan, N. *Eur. J. Inorg. Chem.* **2002**, 2999 and literature cited therein. (c) [Rh(cod)(NN)]$^+$ with NN = monodentate or bidentate amines as precursors of hydroamination catalysts: Beller, M.; Trauthwein, H.; Eichberger, M.; Breindl, C.; Müller, T. E. *Eur. J. Inorg. Chem.* **1999**, 1121. (d) Beller, M.; Trauthwein, H.; Eichberger, M.; Breindl, C.; Müller, T. E.; Zapf, A. *J. Organomet. Chem.* **1998**, *566*, 277. (e) Selent, D.; Scharfenberg-Pfeiffer, D.; Reck, G.; Taube, R. *J. Organomet. Chem.* **1991**, *415*, 417. (f) Adenine base complexes: Sheldrick, W. S.; Günther, B. J. *J. Organomet. Chem.* **1991**, *402*, 265. (g) Purine base complexes: Sheldrick, W. S.; Günther, B. J. *J. Organomet. Chem.* **1989**, *315*, 233. (h) A number of crystalline second-sphere complexes between [Rh(cod)$(NH_3)_2$]$^+$ and various crown ethers and cyclodextrins were reported: Colquhoun, H. M.; Doughty, S. M.; Stoddart, J. F.; Slawin, A. M. Z.; Williams, D. J. *J. Chem. Soc., Dalton Trans.* **1986**, 1639 and literature cited therein. (i) Colquhoun, H. M.; Doughty, S. M.; Slawin, A. M. Z.; Stoddart, J. F.; Williams, D. J. *Angew. Chem., Int. Ed. Engl.* **1984**, *24*, 135. (j) Alston, D. R.; Slawin, A. M. Z.; Stoddart, J. F.; Williams, D. J. *Angew. Chem., Int. Ed. Engl.* **1984**, *24*, 787. (k) [IrH_2(tacn)(coe)]Cl (tacn = triazacyclononane): Iimura, M.; Evans, D. R.; Flood, T. C. *Organometallics* **2003**, *22*, 5370 and literature cited therein.

(7) Donkervoort, J. G.; Bühl, M.; Ernsting, J. M.; Elsevier, C. J. *Eur. J. Inorg. Chem.* **1999**, 27 and literature cited therein.

(8) Lappert, M. F.; Power, P. P.; Sanger, A. R.; Srivastava, R. C. *Metal and Metalloid Amides*; Ellis Horwood-Wiley: Chichester, U.K., 1980.

(9) Reviews: (a) Brynzda, H. E.; Tam, W. *Chem. Rev.* **1988**, *88*, 1163. (b) Fryzuk, M. D.; Montgomery, C. D. *Coord. Chem. Rev.*, **1989**, *95*, 1. (c) Fulton, J. R.; Holland, A. W.; Fox, D. J.; Bergman, R. G. *Acc. Chem. Res.* **2002**, *35*, 44.

(10) Recent examples: (a) Tejel, C.; Ciriano, M. A.; Bordonaba, M.; López, J. A.; Lahoz, F. J.; Oro, L. A. *Inorg. Chem.* **2002**, *41*, 2348. (b) Tejel, C.; Ciriano, M. A.; Bordonaba, M.; López, J. A.; Lahoz, F. J.; Oro, L. A. *Chem. Eur. J.* **2002,** *8*, 3128 and literature cited therein. (c) For examples of bridging amides in binuclear rhodium complexes relevant to imine hydrogenation see: Fryzuk, M. D.; Piers, W. E. *Organometallics* **1990**, *9*, 986.

(11) (a) [Ir(NH_2)(Ph)(Cp*)(PMe_3)]: Rais, D.; Bergman, G. R. *Chem. Eur. J.* **2004**, *10*, 3970 and literature cited therein. (b) Krug, C.; Hartwig, J. F. *J. Am. Chem. Soc.* **2004**, *126*, 2694. (c) [MCp*Cl$(NH_2$−R−NTs)]: Murata, K.; Ikariya, T.; Noyori, R. *J. Org. Chem.* **1999**, *64*, 2186. (d) For a three-coordinate Rh(I) β-diiminate olefin complex, see: Budzelaar, P. H. M.; de Gelder, R.; Gal, A. W. *Organometallics* **1998**, 17, 4121. (e) [M(2-$Ph_2PC_6H_4NMe$)(CO)(PPh_3)] (M = Rh, Ir): Dahlenburg, L.; Herbst, K. *J. Chem. Soc., Dalton Trans.* **1999**, 3935. (f) [Ir^{III}-(NR−R′-NR)Cl]: Danopoulos, A. A.; Hay-Motherwell, R. S.; Wilkinson, G.; Cafferkey, S. M.; Sweet, T. K. N.; Hursthouse, M. B. *J. Chem. Soc., Dalton Trans.* **1997**, 3177. (g) [Rh(2-pyridine-carboxamid)(cod)]: Brunner, H.; Nuber, B.; Prommesberger, M. *J. Organomet. Chem.* **1996**, *523*, 179. (h) [Rh(NHAryl)$_2$$(PR_3)_2$]$^-$: Brunet, J.-J.; Commenges, G.; Neibecker, D.; Rosenberg, L. *J. Organomet. Chem.* **1996**, *522*, 117. (i) Rahim, M.; Ahmed, K. J. *Organometallics* **1994**, *13*, 1751.

(12) Rahim, M.; Bushweller, C. H.; Ahmed, K. J. *Organometallics* **1994**, *13*, 4952.

(13) Holland, P. L.; Andersen, R. A.; Bergman, R. G.; Huang, J.; Nolan, S. P. *J. Am. Chem. Soc.* **1997**, *119*, 12800.

(14) K. G. Caulton, *New J. Chem.* **1994**, *18*, 25.

(15) Recent reviews: (a) Alonso, F.; Beletskaya, I. P.; Yus, M. *Chem. Rev.* **2004**, *104*, 3079. (b) Muci, A. R.; Buchwald, S. L. *Top. Curr. Chem.* **2001**, *219*, 131. (c) Hartwig, J. F. *Angew. Chem., Int. Ed.* **1998**, *37*, 2046. (d) Buchwald, S. L. *Acc. Chem. Res.* **1998**, *31*, 805. Recent original papers: (e) Ozerov, O. V.; Guo, C.; Papkov, V. A., Foxman, B. M. *J. Am. Chem. Soc.* **2004**, *126*, 4792 and literature cited therein. (f) Kanzelberger, M.; Zhang, X.; Emge, T. J.; Goldman, A. S.; Zhao, J.; Incarvito, C.; Hartwig, J. F. *J. Am. Chem. Soc.* **2003**, *125*, 13644. For a calculation of a proposed mechanism see: Senn, H. M.; Blöchl, P. E.; Togni, A. *J. Am. Chem. Soc.* **2000**, *122*, 4098.

(16) Recent reviews: (a) Blaser, H.-U.; Malan, C.; Pugin, B.; Spindler, F.; Steiner, H.; Studer, M. *Adv. Synth. Catal.* **2003**, *345*, 103. (b) Noyori, R. *Angew. Chem., Int. Ed.* **2002**, *41*, 2008. (c) Palmer, M. J.; Wills, M. *Tetrahedron: Asymmetry* **1999**, *10*, 2045.

(17) (a) Sandoval, C. A.; Ohkuma, T.; Muñiz, K.; Noyori, R. *J. Am. Chem. Soc.*, **2003**, *125*, 13490 and references cited therein. (b) Noyori, R.; Yamakawa, M.; Hashiguchi, S. *J. Org. Chem.* **2001**, *66*, 7931. (c) Yamakawa, M.; Ito, H.; Noyori, R. *J. Am. Chem. Soc.* **2000**, *122*, 1466.

(18) (a) Ben Cheikh, R.; Bonnet, M. C.; Chaabounni, R.; Dahan, F. *J. Organomet. Chem.* **1992**, *438*, 217. (b) Zahn, I.; Wagner, B.; Polborn, K.; Beck, W. *J. Organomet. Chem.* **1990**, *394*, 601. (c) Krafft, M.; Wilson, L. J.; Onan, K. D. *Organometallics* **1988**, *7*, 2528.

(19) (a) Review: Zassinovich, Mestroni, G.; Gladiali, S. *Chem. Rev.* **1992**, *92*, 1051. (b) Gladiali, S.; Pinna, L.; Delugo, G.; De Martin, S.; Zassinovich, G.; Mestroni, G. *Tetrahedron: Asymmetry* **1990**, *1*, 635.

(20) Zassinovich, G.; Bettella, R.; Mestroni, G.; Bresciani-Pahor, N.; Geremia, S.; Randaccio, L. *J. Organomet. Chem.* **1998**, *370*, 187.

solv = solvent molecule) in these reactions. However, in course of their intensive studies with C_2-symmetric [Rh^I(cod)(diamine)] complexes,[21] Lemaire et al. found strong evidence that amide complexes derived from diamine diolefin complexes such as **E** are directly involved in the catalytic cycle; that is, neither the amine nor the olefin is displaced in the catalytically active species. Likewise, van Leeuwen et al. proposed chiral iridium(I) aminosulfide or aminosulfoxide diene complexes **F** as efficient catalyst precursors in the transfer hydrogenation of aryl alkyl ketones.[22] Dahlenburg et al. investigated rhodium and iridium cod complexes **G** with β-aminophosphanes as ligands as catalysts for the hydrogenation of ketones. While the rhodium complexes were inactive, the iridium amides showed activity and the authors suggested a complex mechanism involving homolytic and heterolytic H_2 cleavage.[23] Theoretical considerations of the catalytic cycle with rhodium(I) complexes of the Lemaire type (**E**) by Sautet[24] suggest that these proceed via a concerted hydrogen transfer with **TS-A** as an energetically low lying transition state (*ML-bi* mechanism).[17] On the other hand, Handgraaf et al. suggest, on the basis of DFT calculations, that the iridium-catalyzed reactions proceed via transition state **TS-B**, in which the alkoxide and the ketone are simultaneously bound (a direct hydrogen transfer mechanism also encountered in the classical Meerwein−Ponndorf−Verley reduction of carbonyl compounds using aluminum isopropoxide as hydrogen transfer agent). In this case, the amine function is not directly involved in the hydrogen transfer step.[25]

On the basis of their findings, Lemaire and Sautet suggested the application of chiral dienes as steering ligands in catalysis.[21a] This concept has been developed independently in other areas of transition-metal-catalyzed reactions.[26−29] Our laboratory reported the synthesis of 5-phosphanyl-5*H*-dibenzo[*a*,*d*]cycloheptenes (tropp)[30] and introduced chirality by asymmetrical substitution at the C=C double bond of the central seven-memberd ring, which has a rigid concave boat conformation.[26] In the following, the 5*H*-dibenzo[*a*,*d*]-cycloheptenyl group is referred to as trop (derived from the trivial name *trop*ylidenyl).

Recently, we isolated the very stable rhodium(I) complexes **H**[31] and **J**[32] with the corresponding bis(5*H*-dibenzo[*a*,*d*]cycloheptene-5-yl)amine, $trop_2NH$, as the ligand. Measurements of the pK_a's of the rhodium(I)-coordinated NH group in dmso gave 20.1(6) for **H** and 18.7(2) for **J**, respectively. These values are remarkably low (about 10 units lower than the pK_a's of free amines) and show that coordination of an amine significantly acidifies the NH function. The bond dissociation energies, BDE, of the coordinated NH functions were estimated to be 380 (**H**) and 361(2) kJ mol^{-1} (**J**). These results prompted us to investigate chiral, tetrachelating, C_2-symmetric bis(trop) diamines as ligands in rhodium(I) and iridium(I) complexes with respect to their performance as phosphane-free transfer hydrogenation catalysts.[33] Because of the rigidity and preorganization of the metal binding site, we expected the formation of especially stable amino−olefin complexes.

Results and Discussion

Syntheses of Ligands and Complexes. The syntheses of the new ligands *N*,*N*′-bis(5*H*-dibenzo[*a*,*d*]-cyclohepten-5-yl)-1,2-diaminocyclohexane ($trop_2$dach) and *N*,*N*′-bis(5*H*-dibenzo[*a*,*d*]cyclohepten-5-yl)-1,2-diphenyl-1,2-ethylenediamine ($trop_2$dpen) is simple and is outlined in Scheme 1. We used the *R*,*R* isomer **1** of 1,2-diaminocyclohexane and the *S*,*S*-configured isomer **2** of 1,2-diphenyl-1,2-diaminoethylene for our experiments. Both starting materials, **1** and **2**, were obtained in enantiomerically pure form according to published procedures.[34,35] Subsequently, these amines were reacted with 2 equiv of 5-chloro-5*H*-dibenzo[*a*,*d*]cycloheptene (**3**), and the resulting *N*,*N*′-bis(trop)-substituted diamines (*R*,*R*)-**4** and (*S*,*S*)-**5** were obtained in excellent yields (>90%).

Rh complexes of ligands (*R*,*R*)-**4** and (*S*,*S*)-**5** were easily prepared (Scheme 1). Stirring of a methylene chloride (CH_2Cl_2) solution of [Rh(cod)$_2$]OTf (OTf$^-$ = triflate, $CF_3SO_3^-$) with 1 equiv of the ligand **4** or **5** for 10 min at room temperature and subsequent addition of *n*-hexane caused almost quantitative precipitation of the desired compounds (*R*,*R*)-**6** and (*S*,*S*)-**7a**, respectively, as air-stable, orange-red, microcrystalline substances. The complex **7b** was synthesized in equally high yield from the less expensive dinuclear complex [Rh$_2$(μ_2-Cl)$_2$(cod)$_2$] as precursor in the presence of $TlPF_6$ in a one-pot procedure. Slow diffusion of *n*-hexane into saturated CH_2Cl_2 solutions of (*R*,*R*)-**6** gave crystals suitable for structure analysis by X-ray diffraction (vide infra). Single crystals of good quality of complex (*S*,*S*)-**7b** were obtained from a saturated acetonitrile solution.

The ^{1}H NMR data of **4** and **5** indicate that these compounds exist as mixtures of at least two different

(21) (a) Bernard, M.; Guiral, V.; Delbecq, F.; Fache, F.; Sautet, P.; Lemaire, M. *J. Am. Chem. Soc.* **1998**, *120*, 1441. (b) Gamez, P.; Fache, F.; Mangeney, P.; Lemaire, M. *Tetrahedron Lett.* **1993**, *34*, 6897. (c) Gamez, P.; Fache, F.; Lemaire, M. *Tetrahedron: Asymmetry* **1995**, *6*, 705. (d) Touchard, F.; Gamez, P.; Fache, F.; Lemaire, M. *Tetrahedron Lett.* **1997**, *38*, 2275. (e) A quantitative experimetal kinetic analysis of the Lemaire system is given by: Bellefon, C.; Tanchoux, N. *Tetrahedron: Asymmetry* **1998**, *9*, 3677.

(22) Petra, D. G. I.; Kamer, P. C. J.; Spek, A. L.; Schoemaker, H. E.; van Leeuwen, P. W. N. M. *J. Org. Chem.* **2000**, *65*, 3010.

(23) (a) Dahlenburg, L.; Götz, R. *Eur. J. Inorg. Chem.* **2004**, 888. (b) Dahlenburg, L.; Götz, R. *J. Organomet. Chem.* **2001**, *619*, 88.

(24) (a) Guiral, V.; Delbecq, F.; Sautet, P. *Organometallics* **2000**, *19*, 1589. (b) Guiral, V.; Delbecq, F.; Sautet, P. *Organometallics* **2001**, *20*, 2207.

(25) Handgraaf, J.-W.; Reek, J. N. H.; Meijer, E. J. *Organometallics* **2003**, *22*, 3150 and literature cited therein.

(26) (a) Grützmacher, H.; Deblon, S.; Maire, P.; Schönberg, H. Ger, Offen. DE 101 59 015.6, 2002. (b) Maire, P.; Deblon, S.; Breher, F.; Geier, J.; Böhler, C.; Rüegger, H.; Grützmacher, H. *Chem. Eur. J.* **2004**, *10*, 4198.

(27) (a) Hayashi, T.; Ueyama, K.; Tokunaga, N.; Yoshida, K. *J. Am. Chem. Soc.* **2003**, *125*, 11508. (b) Tokunaga, N.; Otomaru, Y.; Okamoto, K.; Ueyama, K.; Shintani, R.; Hayashi, T. *J. Am. Chem. Soc.* **2004**, *126*, 13584. (c) Shintani, R.; Okamoto, K.; Otomaru, Y.; Ueyama, K.; Hayashi, T. *J. Am. Chem. Soc.* **2005**, *127*, 54.

(28) Fischer, C.; Defieber, C.; Suzuki, T.; Carreira, E. M. *J. Am. Chem. Soc.* **2004**, 126, 1628.

(29) Short review: Glorius, F. *Angew. Chem., Int. Ed.* **2004**, *43*, 3364.

(30) Thomaier, J.; Boulmaâz, S.; Schönberg, H.; Rüegger, H.; Currao, A.; Grützmacher, H.; Hillebrecht, H.; Pritzkow, H. *New J. Chem.* **1998**, *21*, 947.

(31) Büttner, T.; Breher, F.; Grützmacher, H. *Chem. Commun.* **2004**, 2820.

(32) Büttner, T.; Geier, J.; Frison, G.; Harmer, J.; Calle, C.; Schweiger, A.; Schönberg, H.; Grützmacher, H. *Science* **2005**, *307*, 325.

(33) For an example see: Poyatos, M.; Mata, J. A.; Falomir, E.; Crabtree, R. H.; Peris, E. *Organometallics* **2003**, *22*, 1110 and literature cited therein.

(34) Racemate separation of 1,2-cyclohexanediamine: Larrow, J. F.; Jacobsen, E. N.; Gao, Y.; Hong, Y.; Nie, X.; Zepp, C. M. *J. Org. Chem.* **1994**, *59*, 1939.

(35) Synthesis and racemate separation of 1,2-diphenyl-1,2-ethylenediamine: Pikul, S.; Corey, E. J. *Org. Synth.* **1993**, *71*, 22.

Scheme 1. Syntheses of the Amino−Olefins (*R*,*R*)-4 and (*S*,*S*)-5 and the Rhodium(I) Complexes (*R*,*R*)-6, (*S*,*S*)-7a,b, and (*R*,*R*)-6-H

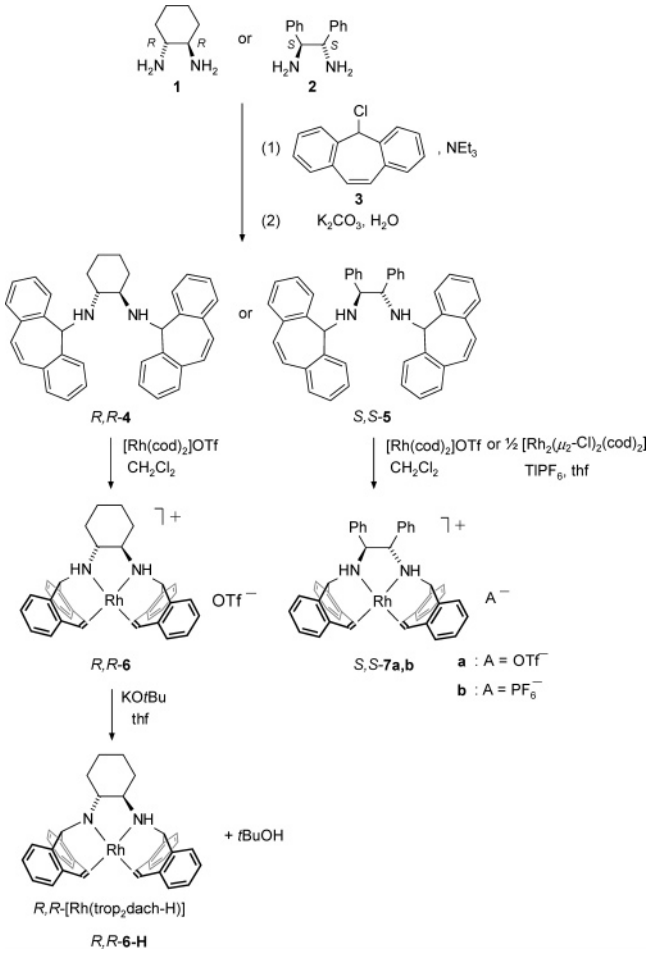

isomers which arise from different inversion isomers with respect to the 5-position of the central seven-membered ring. For the complexes (*R*,*R*)-**6** and (*S*,*S*)-**7a**,**b** only one set of sharp NMR signals is observed, indicating that only one isomer is formed.

The 16-electron complex (*R*,*R*)-[Rh(trop$_2$dach)]OTf ((*R*,*R*)-**6**) is cleanly deprotonated by KO*t*Bu in thf to give the neutral amide complex (*R*,*R*)-[Rh(trop$_2$dach-H)] ((*R*,*R*)-**6-H**) (Scheme 2). The complex (*R*,*R*)-**6-H** was characterized by ^{1}H, ^{13}C, and ^{103}Rh NMR spectroscopy. By slow diffusion of *n*-hexane into a thf solution, red crystals of (*R*,*R*)-**6-H** were obtained, allowing a structure determination by X-ray diffraction.

Reaction of (*S*,*S*)-trop$_2$dpen (**5**) with [Ir$_2$(μ_2-Cl)$_2$(cod)$_2$] in the presence of TlPF$_6$ gave the pale yellow complex **9**, in which only one C=C$_{trop}$ bond of the ligand **5** is bonded to the metal center and one cyclooctadiene (cod) remained complexed (Scheme 2). Even under harsh conditions, that is, refluxing at 110 °C for several hours, we were not able to displace the remaining cod ligand but decomposition was observed instead. Likewise, an attempted hydrogenolysis under 4 bar of H$_2$ failed and no reaction was observed. Similar observations were made when other tetrachelating bis(trop) ligands were reacted with iridium precursor complexes such as [Ir(cod)$_2$]OTf and [Ir$_2$(μ_2-Cl)$_2$(cod)$_2$].[36,37]

Scheme 2. Syntheses of the Iridium(I) Complexes (*S*,*S*)-8 and (*S*,*S*)-9

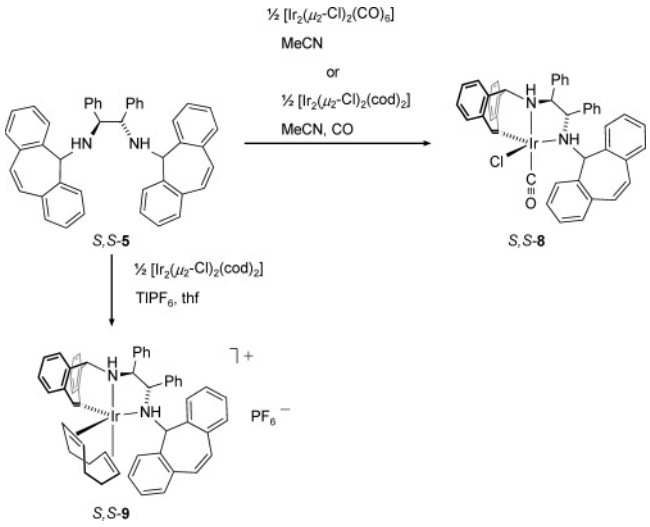

Table 1. Averaged Coordination Chemical Shifts $\Delta\delta_{coord}$ ($=\delta_{complex} - \delta_{free\ ligand}$) in the Cationic 16-Electron Complexes (*R*,*R*)-6, (*S*,*S*)-7a,b, [M(tropdad)]$^+$ (M = Rh, Ir), and *rac*-[M(bis(tropp^{Ph})propane)]$^+$ (M = Rh, Ir), the Neutral Rhodium(I) Amide [Rh(trop$_2$dach-H)] ((*R*,*R*)-6-H), and the 18-Electron Complex [IrCl(CO)(trop$_2$dpen)] ((*S*,*S*)-8)

	^{1}H $\Delta\delta_{coord}$ C*H*=C*H*$_{trop}$ (ppm)	^{13}C $\Delta\delta_{coord}$ C*H*=C*H*$_{trop}$ (ppm)
(*R*,*R*)-[Rh(trop$_2$dach)]$^+$ ((*R*,*R*)-***6***)	−1.77	−53.5
S,*S*-[Rh(trop$_2$dpen)]$^+$ ((*S*,*S*)-**7a**,**b**)	−1.75	<−40
[Rh(tropdad)]$^+$	−1.46	−46.6[b]
[Ir(tropdad)]$^+$	−1.09	−57.4[b]
rac-[Rh{bis(tropp^{Ph})propane}]$^+$	0.42	−32.4
rac-[Ir{bis(tropp^{Ph})propane}]$^+$	−0.93	−43.8
(*R*,*R*)-[Rh(trop$_2$dach-H)] (**6-H**)	−2.64	−58.5
(*S*,*S*)-[IrCl(CO)(trop$_2$dpen)] ((*S*,*S*)-**8**)	−2.97	−102.7[a]

[a] With respect to the ^{13}C chemical shifts of the uncoordinated C=C$_{trop}$ unit (δ 128.9, 130.9). [b] Due to the poor solubility of the free diazadiene ligand, the ^{13}C chemical shifts of the C=C$_{trop}$ units could not be detected in the one-dimensional ^{13}C spectrum. However, they were measured in a ^{1}H−^{13}C correlated spectrum.

Likewise, the reaction of (*S*,*S*)-**5** with the chloro-bridged binuclear iridium carbonyl complex [Ir$_2$(μ_2-Cl)$_2$-(CO)$_6$] afforded the pentacoordinated iridium complex (*S*,*S*)-[IrCl(CO)(trop$_2$dpen)] ((*S*,*S*)-**8**) as a pale yellow microcrystalline powder in which again only one C=C$_{trop}$ entity is bound to the metal. The same complex is obtained in good yield (75%) when the considerably less expensive precursor complex [Ir$_2$(μ_2-Cl)$_2$(cod)$_2$] is reacted with (*S*,*S*)-**5** in acetonitrile (MeCN) under an atmosphere of CO.

NMR Data. The coordination shifts, $\Delta\delta_{coord} = \delta_{complex} - \delta_{ligand}$, caused by coordination of the olefinic units are listed in Table 1. For comparison, we list also the data for the [M(tropdad)]$^+$ complexes[38] and *rac*-[M{bis-(tropp^{Ph})propane}]$^+$ (M = Rh, Ir),[39] shown in Chart 2.

(36) Laporte, C.; Böhler, C.; Schönberg, H.; Grützmacher, H. *J. Organomet. Chem.* **2002**, *641*, 227.
(37) Laporte, C.; Büttner, T.; Rüegger, H.; Geier, J.; Schönberg, H.; Grützmacher, H. *Inorg. Chim. Acta* **2004**, *357*, 1931.
(38) Breher, F.; Böhler, C.; Frison, G.; Harmer, J.; Liesum, L.; Schweiger, A.; Grützmacher, H. *Chem. Eur. J.* **2003**, *9*, 3859.
(39) Laporte, C.; Breher, F.; Geier, J.; Harmer, J.; Schweiger, A.; Grützmacher, H. *Angew. Chem., Int. Ed.* **2004**, *43*, 2567.

Chart 2. Structures of [M(tropdad)]$^+$ (K) and [M{bis(tropp^{Ph})propane}]$^+$ (L) (M = Rh, Ir)

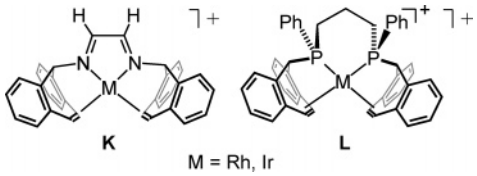

It is assumed that a shift to lower frequencies of ligand resonances indicates increased metal-to-ligand (M→L) back-donation and, hence, significant metallacyclopropane character for the metal−olefin interaction, which raises the metal−ligand binding energy.[40] The $\Delta\delta_{coord}$ values of the ^{1}H and ^{13}C NMR resonances in the cationic complexes (*R*,*R*)-**6** and (*S*,*S*)-**7a**,**b** indicate that the olefins have a strong interaction with the rhodium(I) center. The ^{13}C NMR coordination shifts for the [M(tropdad)]$^+$ complexes are of comparable magnitude. Somewhat lower $\Delta\delta_{coord}$ values are observed for the structurally analogous phosphane complexes *rac*-[M{bis(tropp^{Ph})propane}]$^+$. As expected, $\Delta\delta_{coord}$ values in the neutral amide (*R*,*R*)-**6-H** are more negative (−2.64 in the ^{1}H and −58.5 in the ^{13}C NMR spectrum). The largest $\Delta\delta_{coord}$ value is observed for the pentacoordinated iridium complex [IrCl(CO)(trop$_2$dpen)] ((*S*,*S*)-**8**), where $\Delta\delta_{coord}$ exeeds 100 ppm for the olefinic ^{13}C resonances, while the signals of the noncoordinated C=C$_{trop}$ bond remain unaffected. Given the present data, we conclude that the C=C$_{trop}$ unit in all complexes is tightly bound.

The tetracoordinated rhodium amide complex (*R*,*R*)-**6-H** shows four distinct olefinic resonances in the ^{1}H (2.99, 3.49, 4.29, 4.83 ppm) and ^{13}C NMR spectra (67.0, 67.3, 71.2, 81.4 ppm), indicating that a conceivable proton exchange between the two nitrogen centers is slow on the NMR time scale. Pairwise inequivalent proton resonances of the coordinated CH=CH$_{trop}$ units are expected because of the C_2 symmetry; however, the significant differences of about 1.2 ppm in (*R*,*R*)-**6**, 1.3 in (*R*,*R*)-**6-H**, and 1.18 ppm in (*S*,*S*)-**7a**,**b** point to tetrahedrally distorted coordination spheres[39] (in the free ligands (*R*,*R*)-**4** and (*S*,*S*)-**5**, these differences are only approximately 0.3 ppm). Comparing the NMR data for the cationic complex (*R*,*R*)-**6** with those for neutral (*R*,*R*)-**6-H** suggests there is little change of the gross structural form upon deprotonation of (*R*,*R*)-**6**.

The proton resonances of the NH groups of the ligand are shifted to higher frequency by approximately 2−2.8 ppm upon coordination to the metal, consistent with the observed acidification of these groups (vide infra).

Both of the cationic rhodium(I) complexes (*R*,*R*)-**6** and (*S*,*S*)-**7a**,**b** show similar ^{103}Rh NMR resonances at 917 ppm ((*R*,*R*)-**6**) and 922 ppm ((*S*,*S*)-**7a**,**b**) which lie in the range (750−1060 ppm) determined by Elsevier, Bühl, et al. for a number of [Rh(cod)(N$_2$)]A complexes (N$_2$ = nitrogen donor ligands, A = counteranion).[41] These authors also showed that the ^{103}Rh NMR shift is decisively affected by the Rh−N bond lengths but is affected much less by the N−Rh−N angle or formal oxidation state of the metal center.[42] Specifically, the ^{103}Rh NMR chemical shifts are found at lower frequencies with decreased Rh−N bond lengths. For the amide (*R*,*R*)-**6-H** we find $\delta(^{103}Rh)$ 736 ppm; that is, a shielding of about 200 ppm relative to (*R*,*R*)-**6**, which indicates that the averaged Rh−N bond distances shorten upon deprotonation (vide infra).

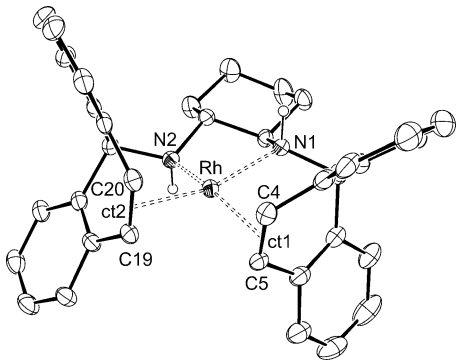

Figure 1. Structure of the cation (*R*,*R*)-[Rh(trop$_2$dach)]$^+$ in (*R*,*R*)-**6**. Thermal ellipsoids are drawn at the 30% probability level; hydrogen atoms (apart from the N*H*), the CF_3SO_3 anion, and the CH_2Cl_2 solvent molecule are omitted for clarity. Selected bond lengths (Å) and angles (deg): Rh−N1 = 2.090(3), Rh−N2 = 2.100(3), Rh−C4 = 2.152(4), Rh−C5 = 2.105(4), Rh−ct1 = 2.011(4), Rh−C19 = 2.145(4), Rh−C20 = 2.093(3), Rh−ct2 = 1.997(4), C4=C5$_{trop}$ = 1.399(6), C19=C20$_{trop}$ = 1.416(6); N1−Rh−N2 = 82.9(1), N1−Rh−ct1 = 91.8(1), N2−Rh−ct2 = 92.1(1), ct1−Rh−ct2 = 97.3(2); Σ°(N1) = 341.0(1)°; Σ°(N2) = 339.0(1)°; φ = 21.7°. ct denotes the centroids of the C=C$_{trop}$ units; φ is the intersection of the planes spanned by the rhodium atom, the N atom, and ct of each bis-chelate ligand.

Structures of (*R*,*R*)-6, (*S*,*S*)-7b, (*R*,*R*)-6-H, and (*S*,*S*)-8. The structures of the cationic tetracoordinated 16-electron rhodium(I) complexes (*R*,*R*)-**6a** and (*S*,*S*)-**7b**, the neutral amide (*R*,*R*)-**6-H**, and the pentacoordinate 18-electron iridium complex (*S*,*S*)-**8** were determined by X-ray diffraction studies. The results are displayed in Figures 1−4; details concerning the data collection and refinement are given in Table 3 in the Experimental Section. We list only selected averaged bond lengths and angles in the figure captions.

The structures of the complex cations in (*R*,*R*)-**6** and (*S*,*S*)-**7b** are very similar (see Figures 1 and 2). Both contain puckered five-membered RhN$_2$C$_2$ chelate rings with N−Rh−N bite angles in the typical range of 81−83°.[41] Also, the Rh−N (average 2.09 Å), Rh−C (average 2.13 Å), and Rh−ct (average 2.01 Å) distances are almost identical (±0.02 Å) (ct = centroid of the coordinated C=C$_{trop}$ bond). Both complexes show, as expected on the basis of the ^{1}H NMR data, moderately tetrahedrally distorted coordination spheres around the rhodium atoms (φ = 21.7°, (*R*,*R*)-**6**; φ = 20.1°, (*S*,*S*)-**7b**).[42] The coordinated olefinic bonds show the expected elongation from about 1.33 Å in the free ligands[30,36] to approximately 1.41 Å in the complexes. Two acetonitrile molecules are hydrogen bonded at a distance of about 2.17 Å to the N1H and N2H functions. Similar hydrogen bonding in the second coordination sphere has been

(40) (a) Frenking, G.; Wichmann, K.; Fröhlich, N.; Loschen, C.; Lein, M.; Frunzke, J.; M. Rayón, V. *Coord. Chem. Rev.* **2003**, *238*−*239*, 55. (b) Frison, G.; Grützmacher, H.; Frenking, G. Unpublished results.

(41) Donkervoort, J. G.; Bühl, M.; Ernsting, J. M.; Elsevier, C. J. *Eur. J. Inorg. Chem.* **1999**, 27 and literature cited therein.

(42) The following reference cites some tetrahedrally distorted rhodium(I) complexes and discusses the influence of geometrical and electronic parameters on the ^{103}Rh resonances: Leitner, W.; Bühl, M.; Fornika, R. Six, C.; Baumann, W.; Dinjus, E.; Kessler, M.; Krüger, C.; Rufińska, A. *Organometallics* **1999**, *18*, 1196.

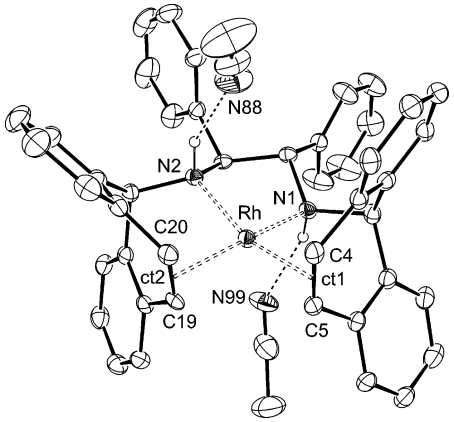

Figure 2. Structure of the cation (*S*,*S*)-[Rh(trop$_2$dpen)]$^+$·2CH$_3$CN in (*S*,*S*)-**7b**. Thermal ellipsoids are drawn at the 30% probability level; hydrogen atoms (apart from the N*H*) and the PF_6 anion are omitted for clarity. Selected bond lengths (Å) and angles (deg): Rh−N1 = 2.093(3), Rh−N2 = 2.083(3), Rh−C4 = 2.103(4), Rh−C5 = 2.157(4), Rh−ct1 = 2.012(4), Rh−C19 = 2.102(4), Rh−C20 = 2.176(4), Rh−Ct2 = 2.019(4), C4═C5$_{trop}$ = 1.400(6), C19═C20$_{trop}$ = 1.412(6); N1−Rh−N2 = 81.1(1), N1−Rh−ct1 = 92.3(1), N2−Rh−ct2 = 92.1(1), ct1−Rh−ct2 = 98.2(2); Σ°(N1) = 342.7(1)°; Σ°(N2) = 339.7(1)°; φ = 20.1°. ct denotes the centroids of the C═C$_{trop}$ units; φ is the intersection of the planes spanned by the rhodium atom, the N atom, and ct of each bis-chelate ligand.

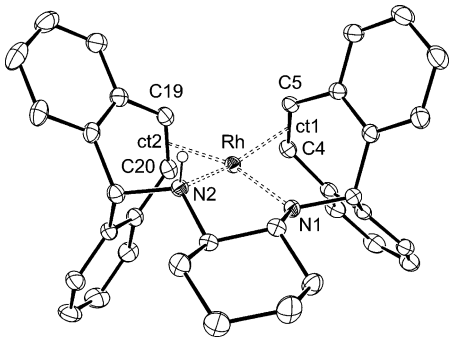

Figure 3. Structure of (*R*,*R*)-[Rh(trop$_2$dach-H)] ((*R*,*R*)-**6-H**). Thermal ellipsoids are drawn at the 30% probability level; hydrogen atoms (apart from the N*H*) and two thf solvent molecules are omitted for clarity. Selected bond lengths (Å) and angles (deg): Rh−N1 = 1.962(2), Rh−N2 = 2.110(2), Rh−C4 = 2.129(2), Rh−C5 = 2.114(2), Rh−ct1 = 1.999(2), Rh−C19 = 2.151(2), Rh−C20 = 2.104(2), Rh−ct2 = 2.007(2), C4═C5$_{trop}$ = 1.421(4), C19═C20$_{trop}$ = 1.416(4); N1−Rh−N2 = 82.30(8), N1−Rh−ct1 = 92.21(9), N2−Rh−ct2 = 91.98(9), ct1−Rh−ct2 = 97.8(1); Σ°(N1) 351.1(2)°; Σ°(N2) 337.4(2)°; φ = 22.2°. ct denotes the centroids of the C═C$_{trop}$ units, Σ°(N) denotes the sum of the bond angles at the nitrogen atoms, and φ is the intersection of the planes spanned by the rhodium atom, the N atom, and ct of each bis-chelate ligand.

intensively studied in supramolecular host−guest chemistry with [Rh(NH$_3$)$_2$(cod)]$^+$ complexes.[6h−j]

The structure of the neutral rhodium amide (*R*,*R*)-**6-H** (Figure 3) is of special interest, as it represents the closest analogue to the catalytically active species proposed by Sautet and Lemaire, which is obtained by deprotonation of complex **E** (see Scheme 1). As deduced from the NMR spectra, the amide complex has a tetrahedrally distorted structure (φ = 22.2°) very similar to that of the cationic precursor complex (*R*,*R*)-**6**. The

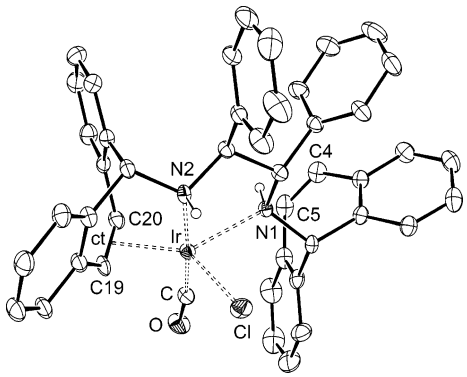

Figure 4. Structure of (*S*,*S*)-[IrCl(CO)(trop$_2$dpen)] ((*S*,*S*)-**8**). Thermal ellipsoids are drawn at the 30% probability level; hydrogen atoms (apart from the N*H*) and a toluene solvent molecule are omitted for clarity. Selected bond lengths (Å) and angles (deg): Ir−N1 = 2.267(3), Ir−N2 = 2.119(3), Ir−Cl = 2.508(1), Ir−C19 = 2.093(4), Ir−C20 = 2.100(4), Ir−ct = 1.964(4), Ir−C = 1.830(4), C−O = 1.135(6), C19═C20$_{trop}$ = 1.468(6), C4═C5$_{trop}$ = 1.372(7); N2−Ir−C = 176.4(2), ct−Ir−Cl = 130.6(1), N1−Ir−Cl = 84.91(8), N1−Ir−ct = 141.5(2); Σ°(N1) = 335.6(1)°; Σ°(N2) = 340.5(1)°. ct denotes the centroid of the C═C$_{trop}$ unit.

rhodium−N1$_{amide}$ bond (1.962(2) Å) belongs to the shortest Rh−N bonds reported to date (see ref 11d for a slightly shorter one) and is 0.15 Å shorter than the rhodium−N2$_{amine}$ bond (2.110(2) Å). Comparable bond shortenings of about 7% were also observed for other pairs of rhodium amine/amide complexes.[4a] As assumed on the basis of the ^{103}Rh NMR shift, the average Rh−N bond distance (2.036(2) Å) is slightly shorter than in (*R*,*R*)-**6** (2.095(3) Å) or (*S*,*S*)-**7b** (2.088(3) Å). The amide nitrogen N1 resides in a slightly pyramidal coordination sphere (Σ° = 351.1(2)°; compare to the sum of the equivalent bond angles around N2, Σ° = 337.4(2)°). Stronger pyramidalized amide nitrogen coordination spheres were observed in the amide complexes obtained by deprotonation of **H** (339.4°) and **J** (341.5°), where the Rh−N bonds were shortened by only about 2%.[31,32] As expected from the more pronounced coordination shifts $\Delta\delta$ in the NMR spectra (see Table 1), the Rh−ct (average 2.00 Å) and Rh−C (average 2.13 Å) bonds in (*R*,*R*)-**6-H** are slightly shorter and the C═C$_{trop}$ bonds (average 1.42 Å) slightly longer than in the cationic protonated precursor complex (*R*,*R*)-**6**. However, a measurable trans influence of the amide is not observed and both C═C$_{trop}$ units are equally bound within the experimental errors.

The structure of the iridium complex (*S*,*S*)-**8** (Figure 4) is best described as a severely distorted trigonal bipyramid with the CO and N2 donor atoms in the apical positions. Both the ct−Ir−Cl and ct−Ir−N1 angles are widened beyond 130° with respect to the ideally expected 120°, while concomitantly the Cl−Ir−N1 angle is acute (84.91(8)°). The overall result of this strong distortion is a Y-shaped arrangement of the ligands in the equatorial plane which was observed for other iridium tropp complexes as well, however, to a lesser extent.[43]

The distance, Ir−ct, of the iridium center to the coordinated C═C$_{trop}$ bond is remarkably short (1.968 Å),

(43) Breher, F.; Rüegger, H.; Mlakar, M.; Rudolph, M.; Deblon, S.; Boulmaâz, S.; Schönberg, H.; Thomaier, J.; Grützmacher, H. *Chem. Eur. J.* **2004**, *10*, 641.

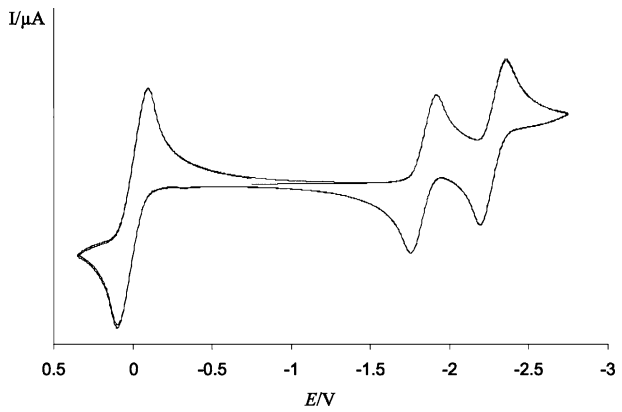

Figure 5. Cyclic voltammogram of (*R*,*R*)-[Rh(trop$_2$dach)]-OTf ((*R*,*R*)-**6a**) in a thf/*n*Bu$_4$NPF$_6$ electrolyte at $T = -25$ °C, at a scan rate of 100 mV s^{-1}.

and the corresponding C=C$_{trop}$ bond (1.501 Å) is the longest we have observed in any trop type complex so far. This is in accord with the very low frequency shifted ^{13}C resonances (26.4, 28.0 ppm) and implies that the solid-state structure is maintained in solution.

Redox Chemistry, p*K*$_a$, and N−H Bond Dissociation Energy of Tetracoordinated Amino−Olefin Rhodium Complexes. Previously, we showed that trop type phosphanes, tropp, are well-suited to stabilize formally low oxidation states at a metal center. Notably, a number of rhodium(0) and iridium(0) complexes were prepared (see ref 43 and literature cited therein). Given that the redox waves are at least quasi-reversible, cyclic voltammograms (CV) can provide valuable information concerning the relative thermodynamic stabilities of the redox-active species. The CV of (*R*,*R*)-[Rh(trop$_2$dach)]-OTf ((*R*,*R*)-**6a**) recorded in a thf/*n*Bu$_4$NPF$_6$ electrolyte at $T = -25$ °C is shown in Figure 5. The complex (*S*,*S*)-**7b** shows a very similar CV. The redox waves of the Fc/Fc$^+$ standard are shown on the left side, and the two redox waves which correspond to the processes (1) and (2) (trop$_2$diamine = trop$_2$dach ((*R*,*R*)-**4**) and trop$_2$dpen

$$d^8\text{-}[Rh^{I}(trop_2diamine)]^+ + e^- \rightarrow d^9\text{-}[Rh^{0}(trop_2diamine)] \quad (1)$$

$$d^9\text{-}[Rh^{0}(trop_2diamine)] + e^- \rightarrow d^{10}\text{-}[Rh^{-I}(trop_2diamine)]^- \quad (2)$$

((*S*,*S*)-**5**) are displayed on the right side. Both redox processes of the amine rhodium complexes are (quasi)-reversible, nicely demonstrating the stabilizing properties of the trop type ligands. At this point we have not undertaken efforts to synthesize and isolate the neutral paramagnetic species (*R*,*R*)-[Rh(trop$_2$dach)]^0 and (*S*,*S*)-[Rh(trop$_2$dpen)]^0 or the rhodates [Rh^{-I}(trop$_2$dach)]$^-$ and [Rh^{-I}(trop$_2$dpen)]$^-$. The redox potentials are listed in Table 2. For comparison, the electrochemical data for the diphosphane diolefin complex [Rh(tropp^{Ph})$_2$]$^+$ [44] (for a sketch of the tropp^{Ph} ligand see Chart 1 with R = Ph, R′ = H), the complex *rac*-[Rh{bis(tropp^{Ph})propane}]$^+$,[39] and the bis(tropp)diazadiene complex [Rh(tropdad)]$^+$ [38] were included (see Chart 2). The complex *rac*-[Rh{bis-(tropp^{Ph})propane}]$^+$ has a tetrahedrally distorted structure ($\varphi = 30°$), as for (*R*,*R*)-**6** and (*S*,*S*)-**7b**. The redox potentials ($E_{1/2}^1 = -1.46$ V; $E_{1/2}^2 = -1.77$ V) of this

Table 2. Half-Wave Potentials $E_{1/2}^1$ and $E_{1/2}^2$ and Potential Difference ΔE ($=E_{1/2}^1 - E_{1/2}^2$) of (*R*,*R*)-6a, (*S*,*S*)-7b, *rac*-[Rh{bis(tropp^{Ph})propane}]$^+$, and [Rh(tropdad)]$^+$ versus Fc/Fc$^+$ at the Scan Rate v = 100 mV s^{-1} [a]

	$E_{1/2}^1$ (V)	$E_{1/2}^2$ (V)	ΔE (V)
(*R*,*R*)-**6a**	−1.83	−2.27	0.44
(*S*,*S*)-**7b**	−1.78	−2.24	0.46
[Rh(tropp^{Ph})$_2$]$^+$ [b]	−1.27	−1.66	0.39
rac-[Rh{bis(tropp^{Ph})propane}]$^+$ [b]	−1.46	−1.77	0.31
[Rh(tropdad)]$^+$ [b]	−0.91	−1.64	0.73

[a] Conditions: working electrode, Pt wire; electrolyte, thf/0.1 M *n*Bu$_4$NPF$_6$. [b] In refs 38 and 39 the redox potentials were referenced vs Ag/AgCl; that is, the values given here are shifted by 352 mV to more negative potentials.

complex are comparable to those of other rhodium trop-phosphane complexes.[36,44,45] In comparison to these, the amino−olefin complexes (*R*,*R*)-**6** and (*S*,*S*)-**7b** have significantly more negative reduction potentials, by about 300−400 mV.

A straightforward explanation for this observation, and in line with the above given arguments used to explain the NMR data, is that amines are less capable of depleting the extra electron density in the reduced complexes (*R*,*R*)-[Rh(trop$_2$dach)]^0 and (*S*,*S*)-[Rh(trop$_2$-dpen)]^0 via metal-to-ligand back-bonding. Hence, these neutral complexes are less stabilized when compared to the complexes containing trop-phosphanes which do act as better π acceptors.[46] On the other hand, the [16 + 1]-electron complex [Rh(tropdad)]^0, containing a "non-innocent" diazadiene ligand serving as a strong electron acceptor, has a significantly less negative first redox potential (−0.91 V vs Fc$^+$/Fc).[38] From the difference, ΔE, of the first and second redox potentials the equilibrium constants K_{disp} were calculated for the disproportionation reactions (3) and (4) to be $K_{disp} = 3.62 \times 10^{-8}$ and 1.7×10^{-8}, respectively.

$$2[Rh^{0}(trop_2dach)] \rightleftarrows [Rh^{I}(trop_2dach)]^+ + [Rh^{-I}(trop_2dach)]^- \quad (3)$$

$$2[Rh^{0}(trop_2dpen)] \rightleftarrows [Rh^{I}(trop_2dpen)]^+ + [Rh^{-I}(trop_2dpen)]^- \quad (4)$$

That is, the paramagnetic 17-electron complexes (*R*,*R*)-[Rh(trop$_2$dach)]^0 and (*S*,*S*)-[Rh(trop$_2$dpen)]^0 are thermodynamically stabilized by about 40 kJ mol^{-1} with respect to the disproportionation into the corresponding diamagnetic 16- and 18-electron complexes. This stabilization is slightly higher than in the phosphane complex *rac*-[Rh^0{bis(tropp^{Ph})propane}] (∼30 kJ mol^{-1}). On the other hand, for the rhodium(0) tropdad complex the disproportionation reaction is endergonic by more than 70 kJ mol^{-1}.

(44) Schönberg, H.; Boulmaâz, S.; Wörle, M.; Liesum, L.; Schweiger, A.; Grützmacher, H. *Angew. Chem., Int. Ed.* **1998**, *37*, 1423.
(45) Deblon, S.; Rüegger, H.; Schönberg, H.; Loss, S.; Gramlich, V.; Grützmacher, H. *New J. Chem.* **2001**, *23*, 83.
(46) An alternative explanation would be that the ground state of the 16-electron complexes (*R*,*R*)-[Rh(trop$_2$dach)]$^+$ and (*S*,*S*)-[Rh(trop$_2$-dpen)]$^+$ are especially stabilized with respect to the reduced neutral complexes and with respect to the redox couples involving rhodium trop-phosphanes. However, because phosphanes certainly act as stronger binding ligands and stabilize a tetracoordinated rhodium(I) complex better than an amine, we consider this situation as less likely.

Scheme 3. Determination of the pK_a of (*R*,*R*)-6 (Eq 5), the Redox Potential of (*R*,*R*)-6-H (Eq 6), and the NH Bond Dissociation Energy (BDE) in (*R*,*R*)-6 (Eq 7)

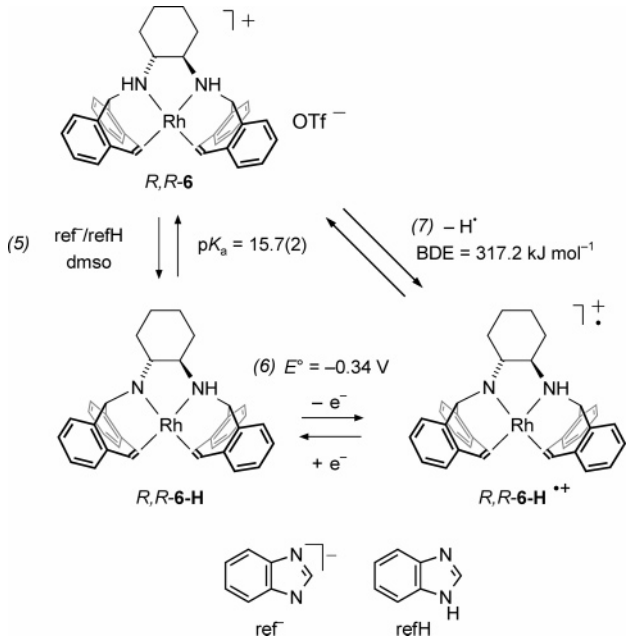

The pK_a value of $[Rh(trop_2dach)]^+OTf^-$ ((*R*,*R*)-**6**) was estimated by reaction with a reference base according to (*R*,*R*)-$\mathbf{6}^+$ + ref^- ⇄ (*R*,*R*)-**6-H** + refH in deuterated dimethyl sulfoxide (dmso[d_6]) as solvent. The benzimidazole/benzimidazolide pair (pK_a = 16.4(1))[47] was used as reference refH/ref^-. The equilibrium constant, K = [(*R*,*R*)-**6-H**][refH]/[(*R*,*R*)-$\mathbf{6}^+$][ref^-], was determined by ^{1}H NMR spectroscopy and used in the equation pK_a((*R*,*R*)-**6**) = pK_a(refH) − log K. The mean value of several measurements gave pK_a((*R*,*R*)-**6**) = 15.7(2). This value is significantly lower (approximately 5 units) than in the pentacoordinated 18-electron rhodium(I) amino olefin complexes **H** and **J** (Chart 1), indicating the rather high acidification of a NH group bonded in a tetracoordinated 16-electron rhodium(I) complex.

In dimethyl sulfoxide (dmso) containing 0.1 M nBu_4NPF_6, the neutral amide complex (*R*,*R*)-[Rh(trop$_2$dach-H)] ((*R*,*R*)-**6-H**) is reversibly oxidized to the radical cation complex (*R*,*R*)-$[Rh(trop_2dach\text{-}H)]^{\bullet+}$ ($[(R,R)\text{-}\mathbf{6\text{-}H}]^{\bullet+}$) at $E°$ = −0.34 V vs Fc/Fc^+. The data of the equilibria (5) ⇄ (6) ⇄ (7) outlined in Scheme 3 are used in the equation BDE = 1.37pK_a + 23.1$E°_{Fc/Fc^+}$ + C (C = 303.5 kJ mol^{-1} for dmso)[48] to estimate the N−H bond dissociation energy in (*R*,*R*)-**6**: BDE = 317(2) kJ mol^{-1}. This bond energy is about 60−70 kJ mol^{-1} lower than in **H** and **J**.

Catalyses. We tested the ability of the trop$_2$dach and trop$_2$dpen complexes to serve as catalyst precursors for the transfer hydrogenation and hydrogenation of acetophenone, which is the standard substrate for this type of reaction.[16,17,19−25] The rhodium complexes (*R*,*R*)-**6** and (*S*,*S*)-**7b** did not show any catalytic activity when they were added to a solution of acetophenone and KO*t*Bu in 2-propanol, and the reaction mixture was kept at 80 °C for 1 h (the ratio, acetophenone:KO*t*Bu:cat was 1:0.1:0.01 in all experiments, which corresponds to frequently applied conditions). The complexes did not decompose under these conditions. Furthermore, the isolated amide (*R*,*R*)-[Rh(trop$_2$dach-H)] ((*R*,*R*)-**6-H**) does not react with dihydrogen even on pressurization to 100 atm. Also, no hydrogenation is observed when (*R*,*R*)-**6-H** is added to acetophenone under an atmosphere of H_2. In all cases, the unreacted amide (*R*,*R*)-**6-H** was observed exclusively in the deep red solutions. A DFT calculation (B3PW91 on the 6-31G* level; see the Supporting Information for further details) with the model amide complex **I** shows that the H_2 addition across the Rh−N bond to yield the rhodium hydride **II** is endothermal by about +26 kJ mol^{-1} (Scheme 4). Furthermore, the reaction proceeds via the energetically high-lying transition state **TS** at 122.5 kJ mol^{-1}, which explains the reluctance of (*R*,*R*)-**6-H** to react with H_2.

Scheme 4. Reaction of Model Rhodium Amide I with H_2 To Give Hydride II

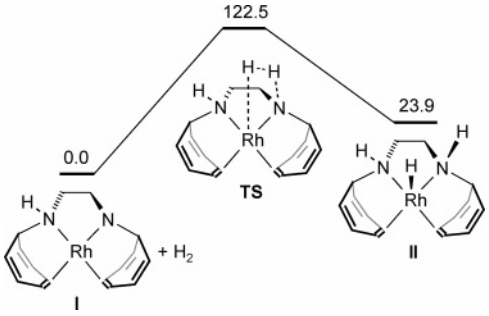

Scheme 5. Transfer Hydrogenation of Acetophenone Catalyzed by the Iridium Complex [IrCl(CO)(trop$_2$dpen)] ((*S*,*S*)-8)

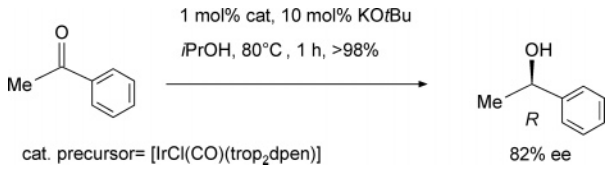

We subsequently tested the pentacoordinated iridium complexes (*S*,*S*)-[IrCl(CO)(trop$_2$dpen)] ((*S*,*S*)-**8**) and $[Ir(cod)(trop_2dpen)]PF_6$ ((*S*,*S*)-**9**) as catalyst precursors under the conditions given above. With (*S*,*S*)-**9** again no reaction occurred, because the complex is too inert and the cod ligand is not displaced. However, with the carbonyl chloride (*S*,*S*)-**8**, complete conversion (>98%) was observed and the *R* isomer of the product 1-phenylethanol was obtained in 82% ee (Scheme 5).

Although it is very speculative at this stage of our investigations, we propose an iridium hydride species, [IrH(CO)(trop$_2$dpen)], as the reactive catalyst in the transfer hydrogenation. This complex can possibly be generated in the following reaction sequence: [IrCl(CO)(trop$_2$dpen)] + O*t*Bu$^-$ → [Ir(CO)(trop$_2$dpen-H)] + *t*BuOH + Cl^-; [Ir(CO)(trop$_2$dpen-H)] + *i*PrOH → [IrH(CO)(trop$_2$dpen)] + Me_2CO. A model for the adduct between this hydride complex and acetophenone is shown in Figure 6. This structure is derived from the experimentally determined structure of (*S*,*S*)-**8** by exchanging the chloride for an hydride (Ir−H = 1.62 Å) and binding an acetophenone molecule via the carbonyl oxygen to the NH group (NH···O = 2.0 Å) and via the carbon of the

(47) Bordwell, F. G. *Acc. Chem. Res.* **1988**, *21*, 456.
(48) Liu, W.-Z.; Bordwell, F. G. *J. Org. Chem.* **1996**, *61*, 4778 and references cited therein.

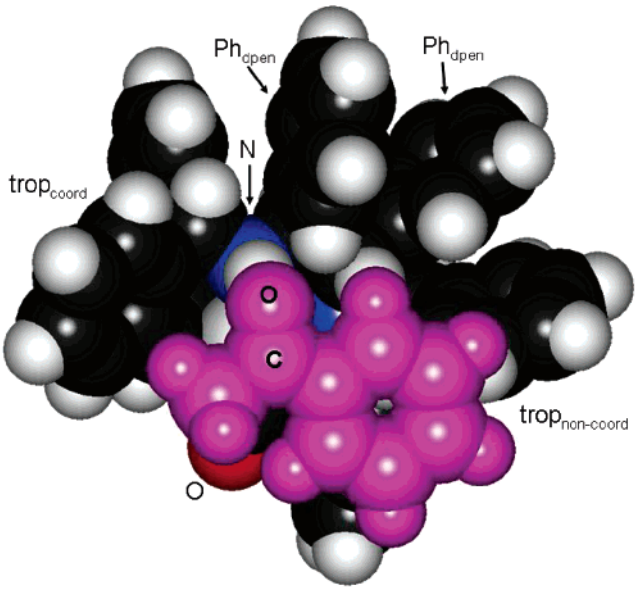

Figure 6. Model of the proposed intermediate {[IrH(CO)(trop$_2$dpen)]·PhMeCO in the transfer hydrogenation of acetophenone catalyzed by (*S*,*S*)-**8** as catalyst precursor.

C═O group to the hydride (IrH···C = 2.5 Å) as typically proposed for these type of intermediates.[24b,25] That is, we assume that the transfer hydrogenation follows the concerted hydrogen transfer path (bifunctional mechanism) via **TS-A** shown in Scheme 1.[16] It has been previously suggested that iridium-catalyzed transfer hydrogenations may follow this as well as the direct hydrogen transfer mechanism.[22] Furthermore, we assume that the hydrogen atom is transferred from the NH group which belongs to the coordinated trop unit.

In our model, this NH group resides in the apical position of the trigonal-bipyramidal coordination sphere of the iridium center. Inspection of a model involving the other NH group in the equatorial position in the hydrogen transfer step would prefer the formation of the *S*-configured isomer of 1-phenylethanol. Unfortunately, we have not yet been able to characterize the products which are formed when (*S*,*S*)-**8** is either reacted with KO*t*Bu alone or with KO*t*Bu/*i*PrOH, whereby complex reaction mixtures are formed.

Conclusions

In one simple step, the new tetrachelating and chiral amino olefins (*R*,*R*)-trop$_2$dach ((*R*,*R*)-**4**) and (*S*,*S*)-trop$_2$dpen ((*S*,*S*)-**5**) were prepared in excellent yield from readily available starting materials. The tetracoordinated 16-electron rhodium(I) complexes (*R*,*R*)-[Rh(trop$_2$dach)]OTf ((*R*,*R*)-**6**) and (*S*,*S*)-[Rh(trop$_2$dpen)]A (A = OTf, (*S*,*S*)-**7a**; A = PF$_6$, (*S*,*S*)-**7b**) were likewise synthesized in high yield as air-stable crystalline solids. With the iridium complexes [Ir$_2$(μ_2-Cl)$_2$(CO)$_6$] and [Ir$_2$(μ_2-Cl)$_2$(cod)$_2$] as precursors, the pentacoordinated 18-electron complexes (*S*,*S*)-[IrCl(CO)(trop$_2$dpen)] ((*S*,*S*)-**8**) and [Ir(cod)(trop$_2$dpen)]OTf ((*S*,*S*)-**9**) were obtained, in which the amino−olefin ligands serve only as tridentate chelate ligands.

The rhodium complexes (*R*,*R*)-**6** and (*S*,*S*)-**7b** can both be reversibly reduced to the corresponding neutral paramagnetic 17-electron complexes [Rh^0(trop$_2$diamine)] and the 18-electron rhodate complexes [Rh^{-I}(trop$_2$diamine)] (trop$_2$diamine = (*R*,*R*)-**4**, (*S*,*S*)-**5**). The observed cathodic shift of the redox potentials in comparison to structurally related phosphane complexes by about 300−400 mV indicates the lack of π-acceptor properties of amines in comparison to phosphanes. When interpreted with the necessary care, such electrochemical data may be of value in order to set qualitative binding arguments in transition-metal chemistry into an experimentally derived quantitative perspective.

The acidic NH function (pK_a = 15.7(2)) of the cationic rhodium complex (*R*,*R*)-[Rh(trop$_2$dach)]$^+$ ((*R*,*R*)-**6**) is easily deprotonated to give quantitatively the neutral rhodium amide complex (*R*,*R*)-[Rh(trop$_2$dach-H)] ((*R*,*R*)-**6-H**). A 7% bond shortening of the Rh−N bond is observed. Although this amide complex is a close analogue to proposed catalysts, it is unreactive in transfer hydrogenations. Also, no reaction is observed between (*R*,*R*)-**6-H** and H$_2$. The structures of the complexes with the tetrachelating amino−olefin ligands described here are very rigid (the complex (*R*,*R*)-[Rh(trop$_2$dach)]OTf does not even contain a rotating side group). We believe that the trigonal-bipyramidal structure of the rhodium hydride complex [RhH(trop$_2$X)] (X = dach, dpen) as intermediate is therefore energetically too disfavored, which shuts down the catalytic cycle. This assumption is bolstered by DFT calculations of model compounds showing that the heterolytic addition of H$_2$ across the Rh−N bond is an endothermic reaction. The structurally more flexible iridium complex (*S*,*S*)-[IrCl(CO)(trop$_2$dpen)] ((*S*,*S*)-**8**) is a suitable precursor complex for a transfer hydrogenation catalyst, and (*R*)-1-phenylethanol is obtained with a respectable 82% ee. This experiment encourages us to continue to search for other phosphane-free hydrogen transfer catalysts having a coordination environment comprised of amino and olefin donor functions and sufficient flexibility in the ligand backbone to allow the easy access of all intermediates in the catalytic cycle.

Experimental Section

General Techniques. All manipulations were performed under an argon atmosphere. Solvents were freshly distilled from sodium/benzophenone (thf, toluene), from sodium/diglyme/benzphenone (*n*-hexane), or from calcium hydride (CH$_2$Cl$_2$, MeCN). Air-sensitive compounds were stored and weighed in a glovebox (Braun MB 150 B-G system), and reactions on a small scale were performed directly in the glovebox. NMR spectra were taken on an Avance DRX-400, Avance DPX-300, or Avance DPX-250 system. The chemical shifts are given as dimensionless δ values and are frequency referenced relative to TMS, CFCl$_3$, H$_3$PO$_4$, and Ξ = 3.16 MHz for ^{1}H and ^{13}C, ^{19}F, ^{31}P, and ^{103}Rh, respectively. Coupling constants *J* are given in hertz (Hz) as positive values regardless of their real individual signs. The multiplicity of the signals is indicated as s, d, or m for singlets, doublets, or multiplets, respectively. The abbreviation br is given for broadened signals. Quaternary carbons are indicated as C_{quat}, aromatic units as CH_{ar}, and cyclohexyl carbons as CH_{cyc} when not noted otherwise. IR spectra were measured with the attenuated total reflection technique (ATR) on a Perkin-Elmer 2000 FT-IR spectrometer in the range from 4000 to 600 cm^{-1} using a KBr beam splitter. The UV/vis spectra were measured with a Perkin-Elmer UV/vis/near-IR Lambda 19 spectrometer in 0.5 cm quartz cuvettes. Mass spectra were taken on a Finnigan MAT 7000 or on an IonSpec HiResESI mass spectrometer.

Syntheses. (*R,R*)-Trop$_2$dach ((*R,R*)-4). To a solution of (*R,R*)-1,2-diammoniumcyclohexane mono-(+)-tartrate (264 mg, 1.00 mmol) in CH_2Cl_2 (15 mL) was added a saturated solution of K_2CO_3 in water (20 mL). After vigorous shaking, the phases were separated, the aqueous phase was extracted twice with CH_2Cl_2 (5 mL), and the combined organic extracts were dried over Na_2SO_4. After filtration, to this solution of free (*R,R*)-1,2-diaminocyclohexane (**1**) was added triethylamine (3 mL) followed by 5-chloro-*5H*-dibenzo[*a*,*d*]cycloheptene (**3**; 454 mg, 2.00 mmol). The stirred solution was heated to reflux for 10 min, and subsequently, the solvent was removed under vacuum. Aqueous workup (CH_2Cl_2/10% K_2CO_3) followed by LC (silica, 1/1 hexanes/Et_2O and then Et_2O) gave (*R,R*)-trop$_2$dach ((*R,R*)-**4**; 444 mg, 0.90 mmol, 90%) as a colorless solid.

NMR spectra in $CDCl_3$ solution show two isomers due to inversion of the seven-membered rings: Symmetric isomer (~43%): ^{1}H NMR (300 MHz, $CDCl_3$) δ 0.54−1.21 (m, 4H, C$H_{2\ cyc}$), 1.37−1.72 (m, 4H, C$H_{2,cyc}$), 1.99−2.16 (m, 2H, CH_{cyc}), 2.26 (br, 2H, NH), 4.79 (s, br, 2H, CH_{benzyl}), 6.58 (d, $^3J_{HH}$ = 11.7 Hz, 2H, CH_{olefin}), 6.78 (d, $^3J_{HH}$ = 11.7 Hz, 2H, CH_{olefin}), 7.12−7.65 (m, 16H, CH_{ar}). Asymmetric isomer (~57%): ^{1}H NMR (300 MHz, $CDCl_3$) δ 0.63−2.34 (m, 10H, C$H_{2\ cyc}$ and CH_{cyc}), 1.95 (br, 1H, NH), 2.85 (br, 1H, NH), 4.21 (d, $^3J_{HH}$ = 3.7 Hz, 1H, CH_{benzyl}), 5.12 (br, 1H, CH_{benzyl}), 7.11−7.66 (m, 20H, CH_{ar} und CH_{olefin}). ^{13}C NMR of both isomers (75 MHz, $CDCl_3$): δ 24.9−32.1 (8C, CH$_{2\ cyc}$), 56.2 (s, 1C, CH$_{benzyl,asym}$), 59.5 (s, 1C, CHN$_{cyc,asym}$), 59.8 (s, 1C, CHN$_{cyc,asym}$), 60.3 (s, 1C, CHN$_{cyc,sym}$), 67.1 (s, 1C, CH$_{benzyl,asym}$), 67.7 (s, 1C, CH$_{benzyl,sym}$), 122.7−134.3 (CH$_{ar}$ and CH$_{olefin}$), 131.5−139.0 (C_{quat}). IR (neat, ATR): ν 3302 m (NH), 3014 m, 2919 m, 1486 m, 1436 s, 1101 m, 798 s, 764 s, 729 s cm^{-1}. EI-MS (70 eV, *m/z*, %): 494 (1), 303 (61), 191 (100), 96 (20). HR-ESI-MS: calcd for $C_{36}H_{35}N_2^+$, 495.2795; found, 495.2788.

(*S,S*)-Trop$_2$dpen ((*S,S*)-5): To a solution of (*S,S*)-1,2-diphenyl-1,2-diaminoethylene (**2**; 313 mg, 1.47 mmol) in CH_2Cl_2 (20 mL) was added triethylamine (5 mL) followed by 5-chloro-*5H*-dibenzo[*a*,*d*]cycloheptene (**3**; 667 mg, 2.95 mmol). The stirred solution was heated to reflux for 10 min, and subsequently the solvent was removed under vacuum. Aqueous workup (CH_2Cl_2/10% K_2CO_3) followed by LC (silica, 3/2 hexanes/Et_2O and then Et_2O) gave (*S,S*)-trop$_2$dpen ((*S,S*)-**5**; 846 mg, 1.43 mmol, 97%) as a colorless foam.

NMR spectra in $CDCl_3$ solution show two isomers due to inversion of the seven-membered rings. Symmetric isomer (~68%): ^{1}H NMR (300 MHz, $CDCl_3$) δ 2.48 (d, $^3J_{HH}$ = 7.8 Hz, 2H, NH), 3.09 (s, 2H, CH_{benzyl}), 4.49 (d, $^3J_{HH}$ = 7.8 Hz, 2H, CH(Ph)(NHtrop)), 6.36 (d, $^3J_{HH}$ = 11.8 Hz, 2H, CH_{olefin}), 6.72 (d, $^3J_{HH}$ = 11.8 Hz, 2H, CH_{olefin}), 6.83−7.47 (m, 26H, CH_{ar}); ^{13}C NMR (75 MHz, $CDCl_3$) δ 65.4 (s, 2C, CH$_{benzyl}$), 66.4 (s, 2C, CH(Ph)(NHtrop)), 126.7 (s, 2C, CH$_{ar}$), 126.8 (2C, CH$_{ar}$), 126.9 (s, 2C, CH$_{ar}$), 127.6 (s, 2C, CH$_{ar}$), 128.0 (s, 4C, CH$_{ar}$), 128.2 (s, 4C, CH$_{ar}$), 128.6 (s, 2C, CH$_{ar}$), 129.3 (s, 2C, CH$_{ar}$), 129.8 (s, 2C, CH$_{ar}$), 129.9 (s, 2C, CH$_{ar}$), 130.0 (s, 2C, CH$_{ar}$), 130.2 (s, 2C, CH$_{olefin}$), 130.3 (s, 2C, CH$_{olefin}$), 133.6 (s, 2C, C$_{quat}$), 133.8 (s, 2C, C$_{quat}$), 139.3 (s, 2C, C$_{quat}$), 140.1 (s, 2C, C$_{quat}$), 141.0 (s, 2C, C$_{quat}$). Asymmetric isomer (~32%): ^{1}H NMR (300 MHz, $CDCl_3$): δ 2.78 (br, 1H, NH), 3.13 (br, 1H, NH), 3.37 (d, $^3J_{HH}$ = 7.0 Hz, 1H, CH(Ph)(NHtrop)), 3.74 (s, 1H, CH_{benzyl}), 3.74 (d, $^3J_{HH}$ = 7.0 Hz, 1H, CH(Ph)(NHtrop)), 4.74 (d, $^3J_{HH}$ = 5.1 Hz, 1H, CH_{benzyl}), 6.82−7.38 (m, 29H, CH_{ar} and CH_{olefin}) 7.70 (d, $^3J_{HH}$ = 7.8 Hz, 1H, CH_{ar}). IR (neat, ATR): ν 3317 m (NH), 3020 m, 1599 w, 1489 m, 1451 s, 1436 s, 1071 m, 797 s, 760 s, 697 s cm^{-1}. EI-MS (70 eV, *m/z*, %): 538 (44), 476 (50), 296 (27), 207 (18), 191 (100). HR-ESI-MS: calcd for $C_{44}H_{37}N_2^+$, 593.2951; found, 593.2943.

(*R,R*)-[Rh(trop$_2$dach)]SO$_3$CF$_3$ ((*R,R*)-6). A red solution of (*R,R*)-trop$_2$dach ((*R,R*)-**4**; 149 mg, 0.30 mmol) and [Rh(cod)$_2$]-SO_3CF_3 (140 mg, 0.30 mmol) in CH_2Cl_2 (3 mL) was stirred for 1 h at room temperature and then layered with *n*-hexane (15 mL). Red crystals of (*R,R*)-[Rh(trop$_2$dach)]SO_3CF_3·CH_2Cl_2 ((*R,R*)-**6**·CH_2Cl_2; 225 mg, 0.271 mmol, 90%) grew overnight. The solvent was decanted, and the product was dried under vacuum.

Mp: >230°C dec. ^{1}H NMR (300.1 MHz, CD_3CN): δ 0.81−1.15 (m, 4H, C$H_{2\ cyc}$), 1.61−1.78 (m, 2H, C$H_{2\ cyc}$), 2.02−2.09 (m, 2H, CH_{cyc}), 2.53 (d, br, $^3J_{HH}$ = 10.3 Hz, 2H, C$H_{2\ cyc}$), 4.16 (d, $^3J_{HH}$ = 9.0 Hz, 2H, CH_{olefin}), 4.45 (d, $^3J_{HH}$ = 9.8 Hz, 2H, NH), 5.10 (d, $^3J_{RhH}$ = 1.9 Hz, 2H, CH_{benzyl}), 5.38 (dd, $^3J_{HH}$ = 9.0, $^2J_{RhH}$ = 1.9 Hz, 2 H, CH_{olefin}), 7.28−7.52 (m, 12H, CH_{ar}), 7.69−7.83 (m, 4H, CH_{ar}). ^{13}C NMR (75.5 MHz, CD_3CN): δ 24.0 (s, 2C, CH$_{2\ cyc}$), 29.4 (s, 2C, CH$_{2cyc}$), 61.7 (s, 2C, CH$_{benzyl}$), 62.4 (s, 2C, CH$_{cyc}$), 70.1 (d, $^1J_{RhC}$ = 11.3 Hz, 2C, CH$_{olefin}$), 83.4 (d, $^1J_{RhC}$ = 13.1 Hz, 2C, CH$_{olefin}$), 127.2 (s, 2C, CH$_{ar}$), 128.1 (s, 2C, CH$_{ar}$), 128.7 (s, 2C, CH$_{ar}$), 129.0 (s, 2C, CH$_{ar}$), 129.0 (s, 2C, CH$_{ar}$), 129.5 (s, 2C, CH$_{ar}$), 129.9 (s, 2C, CH$_{ar}$), 130.0 (s, 2C, CH$_{ar}$), 135.4 (d, J_{RhC} = 0.9 Hz, 2C, C_{quat}), 136.1 (d, J_{RhC} = 2.1 Hz, 2C, C_{quat}), 137.6 (d, J_{RhC} = 1.5 Hz, 2C, C_{quat}), 137.8 (d, J_{RhC} = 1.5 Hz, 2C, C_{quat}). ^{19}F NMR (188.3 MHz, CD_3CN): δ −79.0 (s). ^{103}Rh NMR (12.6 MHz, CD_3CN): δ 922 (s). IR (neat, ATR): ν 3185 w (NH), 3112 w, 2939 w, 1645 w, 1480 m, 1270 s, 1253 vs, 1222 m, 1027 s, 772 m, 756 s cm^{-1}. UV/vis (thf, λ_{max}): 473, 307 nm. ESI-MS (*m/z*, %): 597 (100), [Rh(trop$_2$-dach)]$^+$. Anal. Calcd for $C_{38}H_{36}N_2O_3F_3SCl_2Rh$: C, 54.89; H, 4.36; N, 3.37. Found: C, 54.70; H, 4.44; N, 3.44.

Deprotonation of (*R,R*)-[Rh(trop$_2$dach)]SO$_3$CF$_3$ ((*R,R*)-6) with KO*t*Bu To Give (*R,R*)-[Rh(trop$_2$dach-H)] ((*R,R*)-6-H). To a solution of (*R,R*)-[Rh(trop$_2$dach)]SO_3CF_3 ((*R,R*)-**6**; 30 mg, 0.040 mmol) in thf-d_8 (0.45 mL) was added KO*t*Bu (4.5 mg, 0.040 mmol). The color changed to dark red, and ^{1}H-and ^{13}C NMR spectra were recorded at room temperature.

^{1}H NMR (300.1 MHz, thf-d_8): δ 0.71−0.87 (m, 1H, C$H_{2\ cyc}$), 1.02−1.28 (m, 3H, C$H_{2\ cyc}$), 1.62−1.88 (m, 3H, C$H_{2\ cyc}$ and CH_{cyc}NH), 2.40 (d, $^3J_{HH}$ = 12.5 Hz, 1H, C$H_{2\ cyc}$), 2.44 (d, $^3J_{HH}$ = 12.1 Hz, 1H, C$H_{2\ cyc}$), 2.99 (d, $^3J_{HH}$ = 8.8 Hz, CH_{olefin}), 3.02 (ddd, $^3J_{HH}$ = 12.9 Hz, $^3J_{HH}$ = 12.1 Hz, $^3J_{HH}$ = 3.7 Hz, 1H, CH_{cyc}N), 3.49 (d, $^3J_{HH}$ = 8.8 Hz, 1H, CH_{olefin}), 4.29 (d, $^3J_{HH}$ = 8.8 Hz, 1H, CH_{olefin}), 4.83 (dd, $^3J_{HH}$ = 8.8 Hz, $^2J_{RhH}$ = 2.5 Hz, 1H, CH_{olefin}), 4.96 (s, 1H, CH_{benzyl}), 5.04 (d, $^3J_{RhH}$ = 1.7 Hz, 1H, CH_{benzyl}), 5.07 (d, $^3J_{HH}$ = 12.5 Hz, 1H, NH), 6.86−7.25 (m, 12H, CH_{ar}), 7.38−7.51 (m, 4H, CH_{ar}) (*tert*-butyl alcohol as byproduct with δ 1.19 (s, 9H, CH_3), 3.28 (s, 1H, OH)). ^{13}C NMR (75.5 MHz, thf-d_8): δ 25.0 (s, 1C, CH$_{2\ cyc}$), 25.4 (s, 1C, CH$_{2\ cyc}$), 28.7 (s, 1C, CH$_{2\ cyc}$), 31.6 (s, 1C, CH$_{2\ cyc}$), 62.9 (s, 1C, CH$_{benzyl}$), 64.9 (s, 1C, CH$_{cyc}$NH), 67.0 (d, $^1J_{RhC}$ = 9.4 Hz, 1C, CH$_{olefin}$), 67.3 (d, $^1J_{RhC}$ = 12.0 Hz, 1C, CH$_{olefin}$), 67.9 (s, 1C, CH$_{benzyl}$), 70.2 (s, 1C, CH$_{cyc}$N), 71.2 (d, $^1J_{RhC}$ = 10.7 Hz, 1C, CH$_{olefin}$), 81.4 (d, $^1J_{RhC}$ = 16.9 Hz, 1C, CH$_{olefin}$), 124.0 (s, 1C, CH$_{ar}$), 124.0 (s, 1C, CH$_{ar}$), 124.1 (s, 1C, CH$_{ar}$), 124.4 (s, 1C, CH$_{ar}$), 124.8 (s, 1C, CH$_{ar}$), 125.3 (s, 1C, CH$_{ar}$), 125.6 (s, 1C, CH$_{ar}$), 125.7 (s, 1C, CH$_{ar}$), 126.1 (s, 1C, CH$_{ar}$), 126.8 (s, 1C, CH$_{ar}$), 127.4 (s, 1C, CH$_{ar}$), 127.6, 1C, CH$_{ar}$), 127.8 (s, 2C, CH$_{ar}$), 128.2 (s, 1C, CH$_{ar}$), 128.3 (s, 1C, CH$_{ar}$), 128.9 (s, 1C, CH$_{ar}$), 136.1 (d, J_{RhC} = 1.2 Hz, 1C, C_{quat}), 136.3 (s, 1C, C_{quat}), 139.2 (d, J_{RhC} = 1.2 Hz, 1C, C_{quat}), 139.3 (d, J_{RhC} = 2.3 Hz, 1C, C_{quat}), 140.6 (d, J_{RhC} = 1.6 Hz, 1C, C_{quat}), 142.2 (d, J_{RhC} = 1.4 Hz, 1C, C_{quat}), 145.8 (d, J_{RhC} = 1.2 Hz, 1C, C_{quat}), 150.8 (d, J_{RhC} = 2.0 Hz, 1C, C_{quat}) (*tert*-butyl alcohol as byproduct with δ 30.8 (s, 4C, CH$_3$), 66.7 (s, 1C, C_{quat})). ^{103}Rh NMR (12.6 MHz, CD_3CN): δ 736 (s).

Replacing the argon in the NMR tube with hydrogen gas (ca. 4 bar) did not change the ^{1}H and ^{13}C NMR spectra.

Mp: >235 °C dec. IR (neat, ATR): ν 3204 m (NH), 2922 m, 2851 m, 1598 w, 1485 m, 1467 m, 1404 w, 1261 s, 1231 s, 1041 m, 983 m, 750 s cm^{-1}. UV/vis (thf, λ_{max}): 516, 366 nm. HR-MALDI-MS: calcd for $C_{36}H_{34}RhN_2^+$, 597.1772; found, 597.1752.

(*S,S*)-[Rh(trop$_2$dpen)]SO$_3$CF$_3$ ((*S,S*)-7a). A deep red solution of (*S,S*)-trop$_2$dpen ((*S,S*)-**5**; 119 mg, 0.20 mmol) and [Rh-(cod)$_2$]SO_3CF_3 (94 mg, 0.20 mmol) in dichloromethane (3 mL) was stirred for 1 h at room temperature and then layered with *n*-hexane (15 mL). Red crystals of (*S,S*)-[Rh(trop$_2$dpen)]SO_3-CF_3·CH_2Cl_2 ((*S,S*)-**7a**·CH_2Cl_2; 173 mg, 0.186 mmol, 93%) grew

overnight. The solvent was decanted, and the product was dried under vacuum.

Mp: >160 °C dec. ^{1}H NMR (300.1 MHz, CD_3CN): δ 3.64 (m, AA′XX′ system, 2H, C*H*(Ph)(NHtrop)), 4.36 (d, $^3J_{HH}$ = 9.0 Hz, 2H, CH_{olefin}), 4.39 (d, $^3J_{RhH}$ = 1.9 Hz, 2H, CH_{benzyl}), 5.05 (m, AA′XX′ system, 2H, N*H*), 5.54 (dd, $^3J_{HH}$ = 9.0 Hz, $^2J_{RhH}$ = 2.0 Hz, 2H, CH_{olefin}), 6.77 (br, 2H, CH_{ar}), 6.85 (dd, $^3J_{HH}$ = 7.4 Hz, $^4J_{HH}$ = 1.3 Hz, 2H, CH_{ar}), 7.11 (dd, $^3J_{HH}$ = 7.4 Hz, $^4J_{HH}$ = 1.3 Hz, 2H, CH_{ar}), 7.23 (ddd, $^3J_{HH}$ = 7.4 Hz, $^3J_{HH}$ = 7.4 Hz, $^4J_{HH}$ = 1.3 Hz, 2H, CH_{ar}), 7.27 (br, 8H, CH_{ar}), 7.42 (ddd, $^3J_{HH}$ = 7.4 Hz, $^3J_{HH}$ = 7.4 Hz, $^4J_{HH}$ = 1.3 Hz, 4H, CH_{ar}), 7.50 (ddd, $^3J_{HH}$ = 7.4 Hz, $^3J_{HH}$ = 7.4 Hz, $^4J_{HH}$ = 1.3 Hz, 2H, CH_{ar}), 7.79 (dd, $^3J_{HH}$ = 7.4 Hz, $^4J_{HH}$ = 1.3 Hz, 2H, CH_{ar}), 7.89 (dd, $^3J_{HH}$ = 7.4 Hz, $^4J_{HH}$ = 1.3 Hz, 2H, CH_{ar}). ^{13}C NMR (75.5 MHz, CD_3CN): δ 64.5 (s, 2C, *C*H$_{benzyl}$), 70.2 (s, 2C, *C*H(Ph)(NHtrop)), 71.5 (d, $^1J_{RhC}$ = 11.0 Hz, 2C, *C*H$_{olefin}$), 84.5 (d, $^1J_{RhC}$ = 13.1 Hz, 2C, *C*H$_{olefin}$), 128.1 (s, 2C, *C*H$_{ar}$), 128.5 (s, 2C, *C*H$_{ar}$), 129.7 (s, 2C, *C*H$_{ar}$), 129.9 (s, 2C, *C*H$_{ar}$), 130.0 (s, 2C, *C*H$_{ar}$), 130.0 (s, 2C, *C*H$_{ar}$), 130.5 (s, 2C, *C*H$_{ar}$), 130.7 (s, 2C, *C*H$_{ar}$), 131.1 (s, 2C, *C*H$_{ar}$), 135.6 (s, 2C, C_{quat}), 135.8 (s, 2C, C_{quat}), 137.3 (d, J_{RhC} = 2.1 Hz, 2C, C_{quat}), 137.9 (d, J_{RhC} = 1.2 Hz, 2C, C_{quat}), 138.7 (d, J_{RhC} = 1.4 Hz, 2C, C_{quat}). Rotation of the two phenyl rings leads to broadened resonances in the ^{1}H and ^{13}C NMR spectra. ^{19}F NMR (188.3 MHz, CD_3CN): δ −79.2 (s). ^{103}Rh NMR (12.6 MHz, CD_3CN): δ 917 (s). IR (neat, ATR): ν 3115 m (NH), 2913 w, 1484 m, 1456 m, 1285 s, 1233 s, 1224 m, 1026 s, 751 m 701 s cm^{-1}. UV/vis (thf, λ_{max}): 470, 305, 276 nm. ESI-MS (*m*/*z*, %): 695 (100), [Rh(trop$_2$dpen)]$^+$. HR-MALDI-MS: calcd for $C_{44}H_{36}RhN_2^+$, 695.1934; found, 695.1913.

(*S*,*S*)-[Rh(trop$_2$dpen)]PF$_6$ ((*S*,*S*)-7b). To a solution of of trop$_2$dpen (**5**; 119 mg, 0.20 mmol) and [Rh$_2$(μ_2-Cl)$_2$(cod)] (49 mg, 0.10 mmol) in thf (3 mL) was added TlPF$_6$ (70 mg, 0.20 mmol). The resulting suspension was stirred for 1 h at room temperature and then filtered over Celite to remove TlCl. The solvent and free cod were removed under vacuum, and the residue was recrystallized from dichloromethane/*n*-hexane to give (*S*,*S*)-[Rh(trop$_2$dpen)]PF$_6$·2CH$_2$Cl$_2$ ((*S*,*S*)-**7b**) (162 mg, 0.160 mmol, 80%) as red needles.

Mp: > 205 °C dec. ^{1}H NMR and ^{13}C NMR spectra were in accord with those of (*S*,*S*)-**7a**. IR (neat, ATR): ν 3157 m (NH), 2913 w, 1483 m, 1456 m, 1009 m, 831 vs, 756 s, 699 s.

(*S*,*S*)-[Ir(Cl)(CO)(trop$_2$dpen)] ((*S*,*S*)-8). A suspension of (*S*,*S*)-trop$_2$dpen ((*S*,*S*)-**5**; 29.6 mg, 0.05 mmol) and [Ir$_2$(μ_2-Cl)$_2$(CO)$_6$] (15.5 mg, 0.05 mmol) in CD_3CN (0.45 mL) was heated to 60 °C for 3 h. Pale yellow crystals of (*S*,*S*)-[Ir(Cl)(CO)(trop$_2$dpen)] ((*S*,*S*)-**8**; 31 mg, 0.036 mmol, 72%) grew upon cooling to room temperature.

In an alternative synthesis, MeCN (5 mL) was added to a vigorously stirred mixture of (*S*,*S*)-trop$_2$dpen ((*S*,*S*)-**5**; 119 mg, 0.20 mmol) and [Ir$_2$(μ_2-Cl)$_2$(cod)$_2$] (67 mg, 0.10 mmol) under an atmosphere of carbon monoxide. The resulting yellow-green solution was filtered, and the solvent was removed under vacuum. Recrystallization of the residue from toluene gave (*S*,*S*)-**8** (127 mg, 0.15 mmol, 75%).

Mp: >165 °C dec. ^{1}H NMR (300.1 MHz, CD_2Cl_2): δ 3.18 (dd, $^3J_{HH}$ = 11.3 Hz, $^3J_{HH}$ = 11.0 Hz, 1H, C*H*(Ph)(NHtrop)), 3.35 (d, $^3J_{HH}$ = 8.3 Hz, 1H, CH_{olefin}), 3.80 (d, $^3J_{HH}$ = 8.3 Hz, 1H, CH_{olefin}), 4.29 (dd, $^3J_{HH}$ = 11.4 Hz, $^3J_{HH}$ = 11.3 Hz, 1H, C*H*(Ph)(NHtrop)), 4.39 (d, $^3J_{HH}$ = 2.0 Hz, 1H, CH_{benzyl}), 5.50 (dd, $^3J_{HH}$ = 11.4 Hz, $^3J_{HH}$ = 2.0 Hz, 1H, N*H*), 5.87 (dd, $^3J_{HH}$ = 11.0 Hz, $^3J_{HH}$ = 10.6 Hz, 1H, N*H*), 5.90 (s, br, 2H, CH_{ar}), 6.44 (d, $^3J_{HH}$ = 7.1 Hz, 1H, CH_{ar}), 6.46 (d, $^3J_{HH}$ = 11.7 Hz, 1H, CH_{olefin}), 6.67 (d, $^3J_{HH}$ = 10.6 Hz, 1H, CH_{benzyl}), 6.65−6.71 (m, 2H, CH_{ar}), 6.79−6.85 (m, 3H, CH_{ar}), 7.05 (ddd, $^3J_{HH}$ = 7.6 Hz, $^3J_{HH}$ = 7.6 Hz, $^4J_{HH}$ = 1.2 Hz, CH_{ar}), 7.11−7.51 (m, 15H, CH_{ar}), 7.16 (d, $^3J_{HH}$ = 11.7 Hz, 1H, CH_{olefin}), 7.61 (d, $^3J_{HH}$ = 7.6 Hz, 1H, CH_{ar}), 7.95 (d, $^3J_{HH}$ = 7.6 Hz, 1H, CH_{ar}). ^{13}C NMR (75.5 MHz, CD_2Cl_2): δ 26.4 (s, 1C, *C*H$_{olefin}$), 28.0 (s, 1C, *C*H$_{olefin}$), 64.1 (s, 1C, *C*H$_{benzyl}$), 70.4 (s, 1C, *C*H$_{benzyl}$), 71.2 (s, 1C, *C*H(Ph)(NHtrop)), 73.5 (s, 1C, *C*H(Ph)(NHtrop)), 124.9 (s, 1C, *C*H$_{ar}$), 125.2 (s, 1C, *C*H$_{ar}$), 126.3 (s, 1C, *C*H$_{ar}$), 127.2 (s, 1C, *C*H$_{ar}$), 127.7 (s, 2C, *C*H$_{ar}$), 127.9 (s, 1C, *C*H$_{ar}$), 128.2 (s, 1C, *C*H$_{ar}$), 128.3 (s, 1C, *C*H$_{ar}$), 128.5 (s, 1C, *C*H$_{ar}$), 128.6 (s, 1C, *C*H$_{ar}$), 128.9 (s, 3C, *C*H$_{ar}$), 128.9 (s, 1C, *C*H$_{olefin}$), 129.0 (s, 1C, *C*H$_{ar}$), 129.0 (s, 1C, *C*H$_{ar}$), 129.1 (s, 1C, *C*H$_{ar}$), 129.1 (s, 1C, *C*H$_{ar}$), 129.2 (s, 1C, *C*H$_{ar}$), 129.4 (s, 1C, *C*H$_{ar}$), 129.7 (s, 1C, *C*H$_{ar}$), 130.9 (s, 1C, *C*H$_{olefin}$), 131.5 (s, 1C, *C*H$_{ar}$), 133.2 (s, 2C, C_{quat}), 133.9 (s, 1C, C_{quat}), 135.2 (s, 1C, C_{quat}), 136.2 (s, 1C, C_{quat}), 136.5 (s, 1C, C_{quat}), 137.9 (s, 1C, C_{quat}), 138.9 (s, 1C, C_{quat}), 139.1 (s, 1C, C_{quat}), 141.2 (s, 1C, *C*O) (rotation of phenyl rings around the C_{ipso}−*C*H(Ph)N bond leads to broadened C_{ortho} and C_{meta} resonances). IR (neat, ATR): ν 3271 m, 3171 w, 3020 w, 1975 vs (CO), 1489 m, 1454 m, 1422 w, 1260 w, 1084 w, 987 m, 936 m, 797 m, 732 s cm^{-1}. MALDI-MS (*m*/*z*, %): 785 (96) [Ir(trop$_2$dpen)]$^+$, 621 (100) [Ir(CO)(tropdpen)]$^+$, 593 (64) [Ir(tropdpen)]$^+$. HR-MALDI-MS: calcd for $C_{44}H_{36}IrN_2^+$, 785.2508; found, 785.2499.

(*S*,*S*)-[Ir(cod)(trop$_2$dpen)]Otf ((*S*,*S*)-9). A solution of (*S*,*S*)-trop$_2$dpen ((*S*,*S*)-**5**) (119 mg, 0.20 mmol) and [Ir$_2$(μ_2-Cl)$_2$(cod)$_2$] (67 mg, 0.10 mmol) in acetonitrile (5 mL) was stirred for 1 h at room temperature. TlPF$_6$ (70 mg, 0.20 mmol) was added, and the suspension was stirred for 1 h. The solvent was removed under vacuum, and the residue was chromatographed through a short plug of silica with MeCN as eluent. The product was then recrystallized from CH_2Cl_2/*n*-hexane to yield (*S*,*S*)-[Ir(cod)(trop$_2$dpen)]Otf ((*S*,*S*)-**9**; 115 mg, 0.11 mmol, 55%) as pale yellow needles.

Mp: >220 °C dec. ^{1}H NMR (300.1 MHz, CD_3CN): δ 1.58−1.71 (m, 1H, C$H_{2\ cod}$), 1.93−2.30 (m, 5H, C$H_{2\ cod}$), 2.37−2.53 (m, 2H, C$H_{2\ cod}$), 2.57−2.64 (m, 1H, CH_{cod}), 3.11 (ddd, $^3J_{HH}$ = 8.5 Hz, $^3J_{HH}$ = 8.5 Hz, $^3J_{HH}$ = 4.8 Hz, 1H, CH_{cod}), 3.38 (ddd, $^3J_{HH}$ = 8.5 Hz, $^3J_{HH}$ = 8.5 Hz, $^3J_{HH}$ = 2.6 Hz, 1H, CH_{cod}), 3.65 (dd, $^3J_{HH}$ = 12.7 Hz, $^3J_{HH}$ = 8.7 Hz, 1H, C*H*(Ph)(NHtrop)), 3.94 (ddd, $^3J_{HH}$ = 6.4 Hz, $^3J_{HH}$ = 6.4 Hz, $^3J_{HH}$ = 1.5 Hz, 1H, CH_{cod}), 4.37 (br, 1H, N*H*), 4.49 (dd, $^3J_{HH}$ = 12.7 Hz, $^3J_{HH}$ = 4.6 Hz, 1H, C*H*(Ph)(NHtrop)), 4.54 (d, $^3J_{HH}$ = 9.3 Hz, 1H, CH_{olefin}), 5.11 (s, 1H, CH_{benzyl}), 5.18 (d, $^3J_{HH}$ = 10.7 Hz, 1H, CH_{benzyl}), 5.31 (d, $^3J_{HH}$ = 7.8 Hz, 1H, CH_{ar}), 5.67 (dd, $^3J_{HH}$ = 9.7 Hz, $^3J_{HH}$ = 9.3 Hz, 1H, N*H*), 5.81 (d, $^3J_{HH}$ = 9.3 Hz, 1H, CH_{olefin}), 6.11 (d, $^3J_{HH}$ = 11.6 Hz, 1H, CH_{olefin}), 6.40 (ddd, $^3J_{HH}$ = 7.6 Hz, $^3J_{HH}$ = 7.6 Hz, $^4J_{HH}$ = 1.3 Hz, 1H, CH_{ar}), 6.45 (d, $^3J_{HH}$ = 7.5 Hz, 1H, CH_{ar}), 6.57 (d, ^3J = 7.6 Hz, 1H, CH_{ar}), 6.76 (dd, $^3J_{HH}$ = 7.6 Hz, $^4J_{HH}$ = 1.2 Hz, 1H, CH_{ar}), 6.98 (tt, $^3J_{HH}$ = 7.5 Hz, $^4J_{HH}$ = 1.1 Hz, 1H, CH_{ar}), 7.05−7.89 (m, 20H, 19 CH_{ar} and 1 CH_{olefin}), 8.23 (d, $^3J_{HH}$ = 7.6 Hz, CH_{ar}). ^{13}C NMR (62.9 MHz, CD_3CN): δ 26.6 (s, 1C, *C*H$_{2\ cod}$), 27.8 (s, 1C, CH$_{2\ cod}$), 35.1 (s, 1C, *C*H$_{2\ cod}$), 35.6 (s, 1C, *C*H$_{2\ cod}$), 54.8 (s, 1C, *C*H$_{olefin}$), 57.6 (s, 1C, *C*H$_{olefin}$), 61.9 (s, 1C, *C*H$_{benzyl}$), 64.1 (s, 1C, *C*H$_{cod}$), 65.1 (s, 1C, *C*H(Ph)(NHtrop)), 67.3 (s, 1C, *C*H$_{cod}$), 72.2 (s, 1C, *C*H$_{benzyl}$), 77.4 (s, 1C, *C*H(Ph)(NHtrop)), 82.2 (s, 1C, *C*H$_{cod}$), 91.3 (s, 1C, *C*H$_{cod}$), 124.9 (s, 1C, *C*H$_{ar}$), 126.8 (s, 1C, *C*H$_{ar}$), 126.9 (s, 1C, *C*H$_{ar}$), 127.0 (s, 1C, *C*H$_{ar}$), 127.5 (s, 1C, *C*H$_{olefin}$), 127.6 (s, 1C, *C*H$_{ar}$), 127.8 (s, 1C, *C*H$_{ar}$), 128.2 (s, 1C, *C*H$_{ar}$), 128.4 (br, 1C, *C*H$_{ar}$), 128.8 (s, 1C, *C*H$_{ar}$), 128.8 (s, 1C, *C*H$_{ar}$), 128.9 (s, 1C, *C*H$_{ar}$), 129.0 (s, 1C, *C*H$_{ar}$), 129.1 (s, 1C, *C*H$_{ar}$), 129.3 (s, 1C, *C*H$_{ar}$), 129.3 (s, 1C, *C*H$_{ar}$), 129.4 (s, 1C, *C*H$_{ar}$), 129.4 (s, 1C, *C*H$_{ar}$), 129.7 (s, 1C, *C*H$_{ar}$), 129.7 (s, 1C, *C*H$_{ar}$), 131.2 (s, 1C, *C*H$_{ar}$), 132.3 (s, 1C, C_{quat}), 133.3 (s, 1C, *C*H$_{olefin}$), 134.0 (s, 1C, C_{quat}), 134.4 (s, 1C, C_{quat}), 134.6 (s, 1C, C_{quat}), 134.9 (s, 1C, C_{quat}), 135.8 (s, 1C, C_{quat}), 136.8 (s, 1C, C_{quat}), 137.1 (s, 1C, C_{quat}), 138.1 (s, 1C, C_{quat}), 139.4 (s, 1C, C_{quat}), (s, 1C, C_{quat}). IR (neat, ATR): ν 3272 w (NH), 3202 w (NH), 3027 w, 2959 w, 1600 w, 1494 m, 1456 m, 1439 w, 1412 w, 1162 m, 1056 m, 928 m, 832 vs, 756 s, 698 s cm^{-1}. ESI-MS (*m*/*z*, %): 893 (100), [Ir(cod)(dpentrop$_2$)]$^+$. HR-MALDI-MS: calcd for $C_{52}H_{48}IrN_2^+$, 893.3447; found, 893.3463.

Catalytic Transfer Hydrogenation. To a solution of (*S*,*S*)-[IrCl(CO)(trop$_2$dpen)] ((*S*,*S*)-**8**; 9.3 mg, 0.01 mmol) in 2-propanol (10 mL) was added acetophenone (120 mg, 1.00 mmol) and KO*t*Bu (11.2 mg, 0.10 mmol), and the solution was stirred for 1 h at 80 °C. GC analysis on a chiral column (Machery Nagel Lipodex E) showed complete conversion to (*R*)-

Table 3. Details Concerning the Data Collection and Refinement of the Structures of (*R,R*)-6, (*R,R*)-6-H, (*S,S*)-7b, and (*S,S*)-8

	(*R,R*)-**6**·CH_2Cl_2	(*R,R*)-**6-H**·2thf	(*S,S*)-**7b**·2acn	(*S,S*)-**8**·(toluene)
formula	$C_{38}H_{36}Cl_2F_3N_2O_3RhS$	$C_{44}H_{49}N_2O_2Rh$	$C_{48}H_{42}F_6N_4PRh$	$C_{52}H_{44}ClIrN_2O$
cryst syst	orthorhombic	orthorhombic	orthorhombic	monoclinic
space group	$P2_12_12_1$	$P2_12_12_1$	$P2_12_12_1$	$P2_1$
Z	4	4	4	2
temp, K	250	200	200	250
D_{calcd}, Mg/m^3	1.556	1.384	1.424	1.543
a, Å	13.277(2)	13.102(1)	10.991(1)	9.858(1)
b, Å	15.354(3)	15.387(1)	17.388(1)	20.272(1)
c, Å	17.415(3)	17.638(1)	22.521(1)	11.175(1)
β, deg				115.000(1)
V, Å^3	3550(1)	3555.9(4)	4304.1(5)	2024.0(2)
μ, mm^{-1}	0.747	0.521	0.499	3.407
cryst dimens, mm	0.70 × 0.31 × 0.25	0.99 × 0.78 × 0.54	0.59 × 0.38 × 0.22	0.44 × 0.37 × 0.14
radiation	Mo Kα; graphite monochromator			
2θ range, deg	$3.86 \le 2\theta \le 56.74$	$3.52 \le 2\theta \le 56.40$	$3.62 \le 2\theta \le 49.42$	$4.50 \le 2\theta \le 56.56$
index ranges	$-15 \le h \le 17$	$-17 \le h \le 14$	$-12 \le h \le 12$	$-13 \le h \le 13$
	$-19 \le k \le 20$	$-14 \le k \le 20$	$-20 \le k \le 20$	$-26 \le k \le 26$
	$-23 \le l \le 23$	$-23 \le l \le 23$	$-26 \le l \le 26$	$-14 \le l \le 14$
total no. of rflns	26 115	25 821	34 064	20 827
no. of unique rflns	8763 (R_{int} = 0.0252)	8862 (R_{int} = 0.0238)	7319 (R_{int} = 0.0338)	9863 (R_{int} = 0.0246)
no. of params/restraints	451/6	442/30	543/0	467/1
GOF on F^2	1.076	1.072	1.072	1.031
R1 (rflns $I > 2\sigma(I)$)	0.0477	0.0328	0.0397	0.0296
wR2 (all data)	0.1336	0.0902	0.1048	0.0789
max/min residual electron density, e/Å^3	1.439/−0.621	0.641/−0.423	0.831/−492	1.330/−1.312

1-phenylethanol with an ee of 82%. ^{1}H NMR (300.1 MHz, $CDCl_3$): δ 1.50 (d, $^3J_{HH}$ = 6.6 Hz, 3H, C*H*$_3$), 3.16 (s, 1H, O*H*), 4.85 (q, $^3J_{HH}$ = 6.6 Hz, 1H, C*H*(CH$_3$)(OH)), 7.33−7.40 (m, 5H, C*H*$_{ar}$). ^{13}C NMR (75.6 MHz, $CDCl_3$): δ 25.1 (s, 1C, *C*H$_3$), 70.1 (s, 1C, *C*H(OH)), 125.4 (s, 2C, *C*H$_{ar}$), 127.3 (s, 1C, *C*H$_{ar}$), 128.3 (s, 2C, *C*H$_{ar}$), 145.9 (s, 1C, C_{quat}). EI-MS (70 eV, *m/z*, %): 122 (64, M$^+$), 107 (100), 105 (25), 79 (93), 77 (76), 51 (23).

Cyclic Voltammetry. Cyclic voltammetric investigations were performed using a Princeton Applied Research potentiostat/galvanostat, Model 263A. The measurements were performed in an apparatus designed by Heinze et al.:[49] working electrode, planar platinum electrode (approximate surface area 0.78 mm^2); reference electrode, silver; counter electrode, platinum wire. At the end of each measurement, ferrocene was added as internal standard for calibration.

X-ray Crystallography. Data collection for the X-ray structure determinations were performed on Bruker APEX diffractometer systems by using graphite-monochromated Mo Kα (0.710 73 Å) radiation and a low-temperature device. Red, rodlike crystals of (*R,R*)-**6**·CH_2Cl_2 suitable for X-ray diffraction were obtained by slow diffusion of *n*-hexane into a CH_2Cl_2 solution. Red single crystals of (*S,S*)-**7b**·2acn were obtained from a saturated acetonitrile solution, whereas red crystals of (*R,R*)-**6-H**·2thf and pale yellow crystals of *S,S*-**8**·(toluene) were obtained by layering a thf ((*R,R*)-**6-H**) or a toluene ((*S,S*)-**8**) solution with *n*-hexane.

All single crystals were mounted in perfluoroether oil on top of a glass fiber and then brought into the cold nitrogen stream of a low-temperature device so that the oil solidified. All calculations were performed on PCs by using the SHELX-TL (version 6.12) and SHELXL-97 software packages. All structures were solved by direct methods and successive interpretation of the difference Fourier maps, followed by full-matrix least-squares refinement (against F^2). Moreover, an empirical absorption correction using SADABS (version 2.03) was applied. All atoms were refined anisotropically, except the toluene solvent molecule of (*S,S*)-**8**. The contribution of the hydrogen atoms, in their calculated positions, was included in the refinement using a riding model. The amine hydrogen atoms could be located in a Fourier difference density map but were restrained to ideal positions during the refinement, using the implemented HFIX riding model for NH groups. Upon convergence, the final Fourier difference map of the reported X-ray structures showed no significant peaks; only some residual electron density was located close to the heavy atom rhodium or iridium (~0.8 Å) or solvent molecules (e.g., CH_2Cl_2 in (*R,R*)-**6** or toluene in *S,S*-**8**).

Relevant data concerning crystallographic data, data collection, and refinement details are compiled in Table 3. Crystallographic data (excluding structure factors) for the structures reported in this paper have been deposited with the Cambridge Crystallographic Data Centre as Supplementary Publication Nos. CCDC 269596 ((*R,R*)-**6**), CCDC 269597 ((*R,R*)-**6-H**), CCDC 269598 ((*S,S*)-**7b**), and CCDC 269599 ((*S,S*)-**8**). These data can be obtained free of charge via www.ccdc.cam.ac.uk/conts/retrieving.html (or from the Cambridge Crystallographic Data Centre, 12 Union Road, Cambridge CB21EZ, U.K.; fax (+44)1223-336-033, e-mail deposit@ccdc.cam.ac.uk).

Acknowledgment is made to the LANXCESS AG and the Swiss National Science Foundation for the support of this work.

Supporting Information Available: Details concerning the computational data (methods, structure plots, and tables of Cartesian coordinates of **I**, **TS**, and **II**) and CIf files giving atomic coordinates and equivalent isotropic displacement parameters, bond distances and angles, anisotropic displacement parameters, and hydrogen coordinates and isotropic displacement parameters for (*R,R*)-**6,** (*S,S*)-**7b**, (*R,R*)-**6-H**, and (*S,S*)-**8**. This material is available free of charge via the Internet at http://pubs.acs.org.

OM0500927

(49) Hinkelmann, K.; Heinze, J.; Schacht, H. T.; Field, J. S.; Vahrenkamp, H. *J. Am. Chem. Soc.* **1989**, *111*, 5078.